

DOI:10.13673/j.pgre.202401050

YANG Daoyong, LI Yunlong, HUANG Desheng. Phase Behaviour and Physical Properties of Alkane Solvent(s)/CO₂/N₂/DME/Water/Heavy Oil Systems under Reservoir Conditions[J]. Petroleum Geology and Recovery Efficiency, 2024, 31(2): 175-208.

Phase Behaviour and Physical Properties of Alkane Solvent(s)/CO₂/N₂/DME/Water/Heavy Oil Systems under Reservoir Conditions

YANG Daoyong^{1*}, LI Yunlong, HUANG Desheng

(1. Energy Systems Engineering, Faculty of Engineering and Applied Science, University of Regina, Regina S4S 0A2, Canada)

Abstract: The hybrid steam-solvent injection has been considered as a promising technique for enhancing heavy oil/bitumen recovery, while its main mechanisms including the heat transferred and dissolution of solvents (e.g., CH₄, C₂H₆, C₃H₈, C₄H₁₀, CO₂, N₂, and DME) into heavy oil/bitumen to reduce its viscosity and swell it are closely related to the phase behaviour of the solvents/water/heavy oil systems. To allow the seamless integration with the existing reservoir simulators, the traditional cubic equations of state (i.e., SRK EOS and PR EOS) have been modified and improved to accurately quantify the phase behaviour and physical properties of the aforementioned systems under equilibrium and nonequilibrium conditions. Firstly, a huge database has been built to develop the corresponding alpha functions by minimizing the deviation between the measured and calculated vapour pressures for water as well as non-hydrocarbon and hydrocarbon compounds available from the public domain. Such obtained alpha functions are further validated with enthalpy of vaporization for pure substances, and then the reduced temperature has been optimized and the eccentric factor has been redefined. Finally, a pressure-implicit strategy has been developed to optimize the binary interaction parameters (BIPs) by treating heavy oil as one pseudocomponent (PC) or multiple PCs. Also, the contributions of each solvent to the aforementioned systems have been compared and analyzed within a consistent and unified framework. In addition to new alpha functions for hydrocarbons and water, respectively, the reduced temperature is found to have its optimum value of 0.59 for the two equations of state (EOSs), while 0.60 is recommended for practical use. Such improved EOSs have been further employed to reproduce the experimentally measured multiphase boundaries (or pseudo-bubble-point pressures), density, viscosity, (mutual) solubility, and preferential mass transfer for the aforementioned mixtures under equilibrium and nonequilibrium conditions. The swelling effect for the heavy oil can be enhanced due to the addition of C₃H₈ and/or C₄H₁₀ or their mixtures into the CO₂ stream. Due to the existence of water, isenthalpic flash leads to more accurate quantification of multiphase boundaries and physical properties for the hybrid solvent-thermal processes. Each component of a binary or ternary gas mixture is found to diffuse preferentially into heavy oil at high pressures and elevated temperatures in the absence and presence of porous media, while each of them is found to exsolve differently from gas-saturated heavy oil under nonequilibrium conditions.

Key words: Phase behaviour; Equation of state; Mass transfer; Heat transfer; Solvents/CO₂/N₂/DME/water/heavy oil systems; Equilibrium and nonequilibrium conditions

1 Introduction

As most light and medium oil fields have gradually depleted, it is difficult to meet the increasing demand for crude oil^[1] and recent attention has been directed towards the exploitation of unconventional resources, such as the huge heavy oil and bitumen reserves^[2]. In Canada, the primary heavy oil reserves

are located on the Alberta-Saskatchewan border, while heavy crude oil production in Alberta was approximately 5 million m³ as of October 2021, up about 10% compared to that of the same period in 2020, accounting for nearly 25% of total crude oil production^[3]. Based on its low recovery factor and technical challenges, such as the high oil viscosity and huge energy consumption, it is difficult to effectively and efficiently recover heavy oil in terms of

Corresponding author: Daoyong Yang

Email: tony.yang@uregina.ca

both technical and economic aspects. By taking advantages of both thermal- and solvent-based methods, the hybrid steam-solvent injection has recently been considered as a promising technique for enhancing heavy oil/bitumen recovery, while the heat transferred and dissolution of solvents (e.g., C_3H_8 , C_4H_{10} , CO_2 , N_2 , and dimethyl ether (DME)) into heavy oil/bitumen to swell it and reduce its viscosity are the main recovery mechanisms^[4-6]. Coinjection of solvents (e.g., C_3H_8 , C_6H_{12} , CO_2 , and DME) with steam results in the reduction of oil viscosity and interfacial tension (IFT) as well as additional oil swelling^[7-11]. In addition, a significantly higher oil recovery factor together with less water consumption can be achieved with the addition of solvents into steam compared to the pure steam injection processes^[8,12]. All of the aforementioned effects are related to the phase behaviour of solvents/ CO_2 /water/heavy oil systems, which is of significance for reservoir simulations, and particularly important for simulating and designing the hybrid steam-solvent processes for field applications. Though CO_2 and alkane solvents are important for enhanced heavy oil recovery (EHOR), limited attempts have been made to examine their synergistic effects on heavy oil recovery, not to mention their phase behaviour and physical properties under equilibrium and nonequilibrium conditions. In addition to the inherent foamy oil phenomenon during primary recovery, nonequilibrium phase behaviours inevitably exist in a gas recovery process when the injected gas (es) are used to artificially induce the foamy oil phenomenon in a heavy oil reservoir^[13]. The existing reservoir simulators based on equilibrium conditions failed to accurately describe the nonequilibrium phase behaviour^[13-15]. Therefore, it is of fundamental and practical importance to quantify the phase behaviour and physical properties of alkane solvent (s)/ CO_2 /water/heavy oil systems under equilibrium and nonequilibrium conditions.

Physically, the solvents available for solvent-only or hybrid methods can vary from a poorly soluble one such as nitrogen or methane^[16-18] to a highly soluble one such as hexane ($n-C_6H_{14}$) or tolu-

ene^[19-20]. Most researchers believe that a heavier solvent performs better in terms of enhancing oil production, although a heavier solvent is more expensive in general. Among the solvents, CO_2 , C_2H_6 , C_3H_8 , and $n-C_4H_{10}$ are found to be moderately soluble in heavy oil and affordable; therefore, they are good candidates for practical uses in solvent-based recovery processes^[17-18,21-27]. Also, DME, a promising water-soluble solvent, has recently been found to be an efficient additive to thermal-based recovery methods^[8,28] because of its first-contact miscibility with hydrocarbons and preferential partitioning from the aqueous phase to the oleic phase after being contacted with reservoir fluids, leading to rapid and strong oil-swelling effect and viscosity reduction^[29-31].

In practice, the introduction of steam and solvents into a heavy oil reservoir results in viscosity reduction due mainly to thermal energy and swelling of the hydrocarbon-rich liquid phase because of solvent dissolution^[32-34]. Recently, numerous attempts have been made to determine the multiphase boundaries for the solvent (s)/water/heavy oil systems under reservoir conditions^[19,22,27,35-38]. Li et al.^[39] determined three-phase liquid-liquid-vapour (L_1L_2V) boundaries for C_3H_8/CO_2 /heavy oil mixture and $n-C_4H_{10}/CO_2$ /heavy oil mixture from both experimental and theoretical aspects, respectively. By proposing a generalized methodology to determine multiphase boundaries and swelling factors of solvent(s)/ CO_2 /heavy oil systems at high pressures and elevated temperatures by treating heavy oil as multiple PCs. Li et al.^[36] determined phase behaviour including phase boundaries, volumes, and compositions of the aforementioned systems in the presence of an aqueous phase by applying two different alpha functions for water and non-water components, respectively. Gao et al.^[27] experimentally measured multiphase boundaries of $n-C_4H_{10}$ /water/bitumen mixtures at temperatures up to $160^\circ C$ and pressures up to 10 MPa. Chen and Yang^[38] developed a new and pragmatic methodology to predict phase boundaries and their types as well as solvent solubilities of solvents-heavy oil/bitumen-water systems in a temperature range of 298-573 K for differ-

ent kinds of heavy oils by using new BIPs in the Peng-Robinson equation of state (PR EOS). Chen et al.^[40] developed new experimental measurements together with a dynamic volume analysis (DVA) method to predict the phase behaviour of C₃H₈/water/heavy oil and CO₂/water/heavy oil systems at pressures up to 20 MPa and temperatures up to 432.3 K, during which effective density is used in the ideal mixing rule.^[41] With a generalized Soave-type α function suitable for the Soave-Redlich-Kwong equation of state (SRK EOS) and PR EOS, Pina-Martinez et al.^[42] achieved significant improvements on the prediction of vapour pressures and/or enthalpies of vaporization and/or saturated-liquid heat capacities, especially for heavy molecules with an acentric factor larger than 0.9.

As for reliable and consistent reservoir simulations, accurate quantification of phase behaviour and physical properties of alkane solvent (s)/CO₂/water/heavy oil systems under different conditions is an essential element, while various attempts have been made to improve the traditional cubic equations of state (CEOSs) including the PR EOS^[43] and the SRK EOS^[44], both of which have been widely used in the petroleum industry because of their simplicity and capability in predicting phase behaviour and physical properties of pure substances and mixtures in both vapour and liquid phases^[45-49]. Various attempts have been made to improve the accuracy and robustness of the traditional EOSs with respect to α function, BIP, reduced temperature, and acentric factor.

To accurately predict the characteristics of a real pure substance deviated from its ideal behaviour, an α function is formulated by matching vapour pressure of the pure substance under various conditions, accounting for molecular attraction and mainly depending on both the reduced temperature and acentric factor^[47-48]. As such, the development of a more suitable and robust α function has an important foundation and practical significance for more accurate simulation of phase behaviour and physical properties in such a highly asymmetric system associated with hydrocarbon mixtures. Numerous efforts have been made to improve the α functions for hydrocarbon

compounds (e. g., methane and ethane) and non-hydrocarbon compounds including water (e. g., methanol and ethanol)^[50-53], respectively. A comprehensive review of the available α functions can be found elsewhere^[42]. Physically, there are three basic requirements that need to be met in improving an α function as (1) it must be finite and positive at all temperatures; (2) equals unity at the critical point; and (3) approaches a finite value as the temperature approaches infinity^[54]. As for a given α function, it is easier to achieve the first two requirements compared to the third one. For example, the traditional Soave-type α functions do not meet the third requirement especially when the reduced temperature is infinitely close to infinity^[44]. According to the suggestion made by Neau et al.^[55-56], the temperature at which the Soave-type α functions start to become larger is usually very high, far beyond the scope of the industrial uses, and thus the third criteria is a little less stringent. The logarithm-type α function was originally proposed by Heyen^[57], and then improved by Trebble and Bishnoi^[45] and Twu et al.^[46-48] to a certain extent. Such a logarithm-type α function can meet the third requirement when the reduced temperature approaches infinity. The application of traditional EOSs has achieved good accuracy in the description of the non-aqueous phase, but the predicted results of the aqueous phase deviated from the experimental measurements due to the extremely small hydrocarbon solubility in water^[58]. Since water inevitably exists in a hybrid steam-solvent process, there is a need to introduce a new kind of α function for the water component to improve the accuracy of the EOSs when evaluating a water-associated system since the initial one in the PR EOS was proposed based on a series of water-free systems^[59]. Thus, Peng and Robinson^[59] updated an α function for water in the PR EOS with the temperature range from 284.8 to 466.1 K. Then, Søreide and Whitson^[60] proposed a modified two-parameter α function to reduce the deviation between the predicted vapour pressure of water and the experimental data to 0.20% while expanding the predicted temperature range to 288.2-598.15 K. Based on

the universal α function proposed by Li and Yang^[49], a modified α function for water has been achieved by Li and Yang^[22] and further expanded the applicable temperature range to 273.16-647.10 K. Zhao et al.^[61] performed comparison calculations and found that the α function developed by Li and Yang^[22] had the minimum deviation of 0.07%, followed by the one proposed by Søreide and Whitson^[60] with a deviation of 1.41%, and the original α function made by Peng and Robinson^[59] with a deviation of 1.50%.

The α function in the PR EOS is also dependent upon the acentric factor, which reflects the deviation of acentricity or non-sphericity of a compound molecule from that of a pure and homogeneous fluid, such as argon and xenon^[62]. With the originally proposed α function, Soave^[44] predicted the vapour pressure at a reduced temperature of 0.7 for each of the acentric factor values ranging from zero to 0.5 with a step of 0.05. Subsequently, Peng and Robinson^[43] improved the α function by minimizing the deviation between the theoretically calculated and the experimentally measured vapour pressures for 14 hydrocarbons (methane, ethane, propane, *i*-butane, *n*-butane, cyclohexane, benzene, *i*-pentane, *n*-pentane, *n*-hexane, *n*-heptane, *n*-octane, *n*-nonane and *n*-decane) and 3 permanent gases (N₂, CO₂, and H₂S). Two years later, Robinson and Peng^[59] updated its original version proposed in 1976 by adding a new equation for substances whose acentric factors are lower than or equal to that of *n*-decane. Meanwhile, Graboski and Daubert^[63] proposed a new α function based on a detailed set of hydrocarbon vapour pressure data compiled by the American Petroleum Institute. Subsequently, Soave^[64] not only proposed a new α function that is more suitable for heavy hydrocarbons based on the vapour pressure generated by the Lee-Kesler equation^[65] but also updated the α function to accurately predict the fugacity coefficients of pure gaseous fluids at high pressures and elevated temperatures. By defining its form in terms of the vapour pressure at a reduced temperature of 0.7, Pitzer et al.^[66] generalized a correlation to accurately predict vapour pressure when the reduced temperature is be-

tween 0.7 and 1.0, but the prediction accuracy is compromised when the reduced temperature is lower than 0.7^[67]. In other words, the acentric factor defined at a reduced temperature of 0.7 can accurately reflect the characteristics of a substance (e.g., carbon dioxide and light hydrocarbons) at a temperature close to 70-100% of its critical temperature; however, it is less accurate at representing the characteristics of a substance (e.g., heavy hydrocarbons) at a temperature usually much lower than 70% of its critical temperature encountered in the industrial applications. In order to improve the prediction accuracy of vapour pressures of heavy hydrocarbons at low temperatures, Twu et al.^[67] modified the definition of the acentric factor at reduced temperature of 0.5 instead of 0.7. Based on the work of Twu et al.^[67], Nji et al.^[68] proposed a new α function to improve the prediction performance of the vapour pressure of heavy hydrocarbons, but its prediction for non-hydrocarbon compounds still needs to be improved. Then, Li and Yang^[49] redefined the reduced temperature at 0.6 to balance the characteristics of both light compounds and heavy hydrocarbons, while Chen and Yang^[69] proved that such a redefinition is theoretically sound.

In addition to the accurate representation of saturation conditions of pure substances with the α function, the accuracy of the CEOS prediction is highly dependent on the appropriately tuned binary interaction parameters (BIPs) and mixing rules^[9-10, 70-72]. As for the attractive term of the CEOS, the BIPs between any two compounds in a vapour-liquid mixture are required for accurately predicting their physical properties under vapour equilibrium conditions^[73]. For two individual components with essentially the same polarity, the BIP value is commonly assumed to be equal or close to zero^[74]. As for a highly asymmetric mixture (e.g., CO₂ and *n*-alkanes) with respect to both molecular size and energetic interactions^[75], the introduction of BIPs enables to perform calculations for the vapour-liquid equilibria (VLE). Due to the fact that hydrocarbon binaries are essentially nonpolar molecules, zero BIP is a plausible approximation. Usually, the BIPs can be obtained by either tuning a

CEOS to reproduce the experimental VLE data or using empirical correlations^[73]. Graboski and Daubert^[63] developed a BIP correlation for systems containing CO₂ and light hydrocarbons from C₁ to C₁₀ on the basis of a modified SRK EOS, while solubility parameters of CO₂ and hydrocarbons are preconditioned. Subsequently, a temperature-dependent BIP correlation for binary mixtures of CO₂-*n*-alkanes (C₁ to C₈, C₁₀, and C₂₀) was proposed for the PR EOS^[76], which is superior to the previously proposed methods^[77]. Elliott and Daubert^[78] introduced the Graboski-Daubert method^[63] to predict the VLE of hydrocarbons with N₂, CO₂, CO, and H₂S. After evaluating and comparing BIPs in five different EOSs, Valderrama et al.^[79] found that BIPs are highly dependent on temperature for the SRK EOS but not obvious for the PR EOS. Gao et al.^[80] proposed a function of the critical temperature and compressibility factor to evaluate BIPs of the PR EOS for light hydrocarbon (C₁-C₁₀) mixtures, which shows a poor accuracy in the critical region. Kordas et al.^[81] then extended the hydrocarbon database from C₁ to C₄₄ including light and heavy *n*-alkanes, branched alkanes, and aromatics. Since Lee and Sun^[82] established a model for the BIPs by applying the van der Waals mixing rule, more BIP correlations have been obtained based on different mixing rules^[70-72]. In addition, a group-contribution method can be utilized to predict the BIP for a pair of components, provided that the knowledge of molecular structure of each substance is known^[83]. Thus, it will be physically difficult to determine the BIPs for heavy oil-involved systems because heavy oil is commonly characterized as PCs with unclear molecular structures. Since it has been found previously that the component as heavy as C₂₀₀ may affect the phase behaviour of heavy oil involved systems^[84], it is necessary to further split the plus fraction into single carbon numbers (SCNs). Accordingly, heavy oil can be defined as PCs by applying the splitting and lumping methods^[74,85]. Although interactions between CO₂ and heavy hydrocarbon components impose a marked impact on CO₂-assisted heavy oil recovery processes, few attempts have been

made to develop BIP correlations between CO₂ and heavy *n*-alkanes, resulting in a poor phase behaviour prediction for such an asymmetric system^[85]. Li et al.^[86] proposed a generalized temperature-dependent BIP correlation to more accurately predict the phase behaviour of the CO₂/heavy *n*-alkane systems, while Xu et al.^[73] proposed a correlation rule with a reduced temperature to predict the BIPs of mixtures containing CO₂/alkanes (C₁-C₁₀) in pseudocritical regions.

In addition to collecting the relevant data in the public domain, the main objective of this work is to summarize and compare the experimental measurements and theoretical calculations on quantifying phase behaviour and physical properties of alkane solvent(s)/CO₂/water/heavy oil systems at various pressures and temperatures. Firstly, the α functions respectively for hydrocarbon compound and water compound in the PR EOS or SRK EOS have been modified and improved to more accurately predict the vapour pressure for pure substances. In addition to optimizing the reduced temperature for the redefined acentric factor, a pressure-implicit strategy has been developed to optimize the BIPs correlations by treating heavy oil as either one PC or multiple PCs. Then, such improved EOSs have been further employed to reproduce the experimentally measured multiphase boundaries (or pseudo-bubble-point pressures), density, viscosity, (mutual) solubility, and preferential mass transfer for the alkane solvent (s)/CO₂/water/heavy oil systems under equilibrium and nonequilibrium conditions.

2 Experimental Database

2.1 Phase Boundary

In this study, the measured phase boundaries together with their types for solvents-heavy oil mixtures (including C₃H₈, C₄H₁₀, CO₂, and DME) in the absence and presence of an aqueous phase are collected from the literature. Table 1 shows the data for a total of 41 feeds^[7,9-10,22,36-37,39,41,87] while “L₁” refers to the high-density oil-rich liquid phase, “L₂” refers to the low-density solvents-rich liquid phase, “V” refers to

the vapor phase, and “A” represents the aqueous phase which is mainly comprised of liquid water. Also, the oil samples for most of the collected data are Lloydminster heavy oil; however, the oil samples of #19 and #20 are Huabei heavy oil whose physical properties can be found elsewhere^[36].

2.2 Swelling Factor

The experimentally measured SFs are collected from the literature^[7,9-10,36-37,88], while the details are provided in Table 2.

2.3 Density

In this study, 1606 measured densities for solvents/heavy oil/bitumen/water systems are collected^[40-41,89]. More specifically, there includes a total of 15 different heavy oils/bitumens and 12 solvents (i. e., CH₄ through *n*-C₇H₁₆, CO₂, N₂, toluene, cyclohexane, and DME) with a temperature range of 288-573 K and a pressure range of 0.1-12.8 MPa, respectively. Detailed information can be found in Table 3^[16-19,24-25,28,90-100].

2.4 Viscosity

A total of 258 measured viscosities for solvents-heavy oil/bitumen/water systems in a temperature range of 287.9-463.4 K and a pressure range of 0.46-10.94 MPa, respectively, are collected from literature and presented in Table 4^[18,24,26,92-93,101]. The light solvents include methane, ethane, propane, *n*-butane, *n*-pentane, N₂ and CO₂, while six commonly used mixing rules (i. e., Arrhenius', Cragoe's, Shu's, Lobe's, double log, and power-law) are examined and compared with the measured viscosities for the aforementioned systems retrieved from the literature.

2.5 Solubility

In addition to solubility data, mutual solubility data have been collected for *n*-alkanes (C₃-C₂₀)-water pairs from the literature^[102-112]. It is important to note that most of the experimentally measured solubility data for *n*-alkane-water pairs are retrieved from the IUPAC (i. e., International Union of Pure and Applied Chemistry) reference manual where comprehensive experimental data from different sources have been critically reviewed and well fitted by solubility

correlations^[102-112]. The remaining experimental data can be found elsewhere^[113], while the details are tabulated in Table 5. Mutual solubility means that a hydrocarbon component can dissolve in aqueous phase and water component can dissolve in a liquid hydrocarbon phase as well. Specifically, X_{HC} denotes hydrocarbon solubility in aqueous phase, while X_w refers to water solubility in liquid hydrocarbon phase.

2.6 Mass Transfer

The experimental data of diffusion tests for alkane solvents/CO₂/heavy oil systems are retrieved from the literature^[114-117], while their compositions and operating conditions for a total of 12 diffusion tests (Feeds #42-#53) are listed in Table 6. With an easier comparison purpose, the data of diffusion coefficients for CO₂, C₃H₈, and *n*-C₄H₁₀ published in the literature are summarized in Table 7^[114-131].

2.7 Nonequilibrium Phase Behaviour

Nonequilibrium phase behaviour of alkane solvent(s)/CO₂/heavy oil systems under reservoir conditions have been collected from literature^[132-135]. Constant pressure decline rate and constant volume expansion rate are two major approaches to reach nonequilibrium conditions for the aforementioned systems, although field production constraints associated with foamy oil make it more complicated.

In this study, the data for alkane solvents/CO₂/heavy oil systems under nonequilibrium conditions are collected from the literature, while the details are tabulated in Table 1. More specifically, there are a total of ten constant composition expansion (CCE) experiments with a constant volume expansion rate (see Feeds #54-#56 in Table 8) and a total of six CCE experiments with a constant pressure decline rate (see Feeds #57-#59 in Table 9). It is worthwhile noting that, apparent critical supersaturation pressure (P_s) is defined as the pressure difference between thermodynamic bubblepoint pressure (P_b) and pseudo-bubblepoint pressure, while the rebound pressure is defined as the difference between pseudo-bubblepoint pressure and the maximum pressure after the pseudo-bubblepoint pressure^[132,136].

Table 1 Compositions of solvents/water/heavy oil systems and measured phase boundaries at different temperatures

Feed No.	Composition, mol%						<i>T</i> , K	Phase boundary, kPa				Reference
	C ₃ H ₈	<i>n</i> -C ₄ H ₁₀	CO ₂	heavy oil	water	DME		L ₁ L ₂ /L ₁ L ₂ V	L ₁ L ₂ V/L ₁ V	L ₁ /L ₁ V	AL ₁ /AL ₁ V	
1	0	0	94.4	5.6	0	0	288.65	5175	5097	—	—	
							298.65	6508	6487	—	—	
							304.95	—	—	—	—	
2	23.6	0	67.2	9.2	0	0	288.95	4640	4305	—	—	[39]
							298.55	5610	5328	—	—	
							309.55	—	—	—	—	
3	0	11.8	83.2	5.0	0	0	288.65	4595	3754	—	—	
							298.65	5560	4750	—	—	
							308.55	6718	5941	—	—	
4	67.3	0	0	32.7	0	0	298.55	—	—	800	—	
							323.95	—	—	1400	—	
							348.35	—	—	2400	—	
							396.15	—	—	5000	—	
5	0	62.0	0	38.0	0	0	298.55	—	—	230	—	
							323.95	—	—	400	—	
							348.35	—	—	700	—	
							396.15	—	—	1700	—	
6	0	82.5	0	17.5	0	0	298.55	—	—	240	—	[7]
							323.95	—	—	450	—	
							348.35	—	—	800	—	
							396.15	—	—	2000	—	
7	55.4	15.8	0	28.8	0	0	298.55	—	—	700	—	
							348.35	—	—	1800	—	
							396.15	—	—	4000	—	
8	58.5	0	0	41.5	0	0	323.85	—	—	1307	—	[22]
9	73.0	0	0	27.0	0	0	323.85	—	—	1531	—	
10	81.9	0	0	18.1	0	0	323.85	—	—	1666	—	
11	58.8	0	0	41.2	0	0	298.85	—	—	805	—	
12	65.6	0	0	34.4	0	0	298.85	—	—	820	—	
13	74.4	0	0	25.6	0	0	298.85	—	—	880	—	
14	67.3	0	0	32.7	0	0	298.85	—	—	865	—	
							323.15	—	—	1445	—	
							348.15	—	—	2339	—	
15	36.2	0	38.6	25.2	0	0	280.45	—	—	3175	—	
							298.85	—	—	4667	—	
							318.75	—	—	6662	—	
16	0	34.3	31.7	34.0	0	0	298.85	—	—	3157	—	
							318.75	—	—	4077	—	
							347.65	—	—	5690	—	
							391.55	—	—	8379	—	

续表

Feed No.	Composition, mol%						T, K	Phase boundary, kPa				Reference
	C ₃ H ₈	n-C ₄ H ₁₀	CO ₂	heavy oil	water	DME		L ₁ L ₂ /L ₁ L ₂ V	L ₁ L ₂ V/L ₁ V	L ₁ /L ₁ V	AL ₁ /AL ₁ V	
17	8.6	0	18.5	14.0	58.9	0	321.55	—	—	—	7706	
							334.35	—	—	—	9376	
							344.95	—	—	—	10624	
							357.95	—	—	—	12220	
							373.15	—	—	—	13927	
18	15.8	0	17.1	12.9	54.3	0	298.95	—	—	—	4018	
							309.95	—	—	—	4881	
							318.25	—	—	—	6239	
							329.85	—	—	—	7651	
19	25.0	0	25.0	50.0	0	0	298.15	—	—	—	2895	[36]
							323.15	—	—	—	3850	
							343.15	—	—	—	4603	
							363.15	—	—	—	5375	
							383.15	—	—	—	6070	
20	6.0	0	6.0	80.0	80	0	298.15	—	—	—	3202	
							323.15	—	—	—	4415	
							343.15	—	—	—	5497	
							363.15	—	—	—	6721	
							383.15	—	—	—	7836	
21	0	0	54.5	45.5	0	0	323.15	—	—	7900	—	
							343.45	—	—	9300	—	
							362.55	—	—	11100	—	
22	0	0	28.0	72.0	0	0	323.95	—	—	3000	—	
							348.35	—	—	3800	—	
							362.75	—	—	4200	—	
23	19.6	16.9	34.1	29.4	0	0	296.45	—	—	4900	—	
							317.65	—	—	6900	—	
							327.85	—	—	8100	—	
24	16.5	14.2	28.8	40.5	0	0	302.55	—	—	4600	—	[37]
							323.85	—	—	6200	—	
							343.05	—	—	7800	—	
25	14.7	12.6	25.6	47.1	0	0	322.05	—	—	5200	—	
							342.95	—	—	6600	—	
							362.85	—	—	8000	—	
26	12.1	10.4	21.2	56.3	0	0	333.75	—	—	4800	—	
							353.75	—	—	5700	—	
							373.35	—	—	6700	—	

续表

Feed No.	Composition, mol%						T, K	Phase boundary, kPa				Reference
	C_3H_8	$n-C_4H_{10}$	CO_2	heavy oil	water	DME		L_1L_2/L_1L_2V	L_1L_2V/L_1V	L_1/L_1V	AL_1/AL_1V	
27	81.9	0	0	18.1	0	0	328.7	—	—	1800	—	
							353.2	—	—	2980	—	
							368.7	—	—	4090	—	
							391.2	—	—	7340	—	
							411.4	—	—	9810	—	
							430.2	—	—	11960	—	
28	12.61	0	0	2.79	84.60	0	353.2	—	—	—	2980	
							368.7	—	—	—	4190	
							391.2	—	—	—	7390	
							411.4	—	—	—	9820	
							430.2	—	—	—	11910	
29	0	0	53.2	46.8	0	0	355.5	—	—	10400	—	
							375.0	—	—	11010	—	
							395.9	—	—	12090	—	
							413.2	—	—	13080	—	
							432.3	—	—	14530	—	
30	0	0	4.66	4.09	91.25	0	375.0	—	—	—	8230	
							395.9	—	—	—	8960	
							413.2	—	—	—	9570	
							432.3	—	—	—	10350	
31	5.1	0	5.1	8.4	81.4	0	352.05	—	—	—	6401	
							364.65	—	—	—	7271	
							375.05	—	—	—	7913	
							399.55	—	—	—	9484	
							421.55	—	—	—	10901	
32	0	0	0	78.8	0	21.2	348.2	—	—	412	—	
							363.2	—	—	521	—	
							378.2	—	—	630	—	
							393.2	—	—	758	—	
							408.2	—	—	885	—	
33	0	0	0	58.4	0	41.6	348.2	—	—	776	—	
							363.2	—	—	1071	—	
							378.2	—	—	1329	—	
							393.2	—	—	1675	—	
							408.2	—	—	1991	—	
34	0	0	0	10.4	82.2	7.4	348.2	—	—	—	956	
							363.2	—	—	—	1284	
							378.2	—	—	—	1701	
35	0	0	0	10.5	78.3	11.2	348.2	—	—	—	1263	
							363.2	—	—	—	1580	
							378.2	—	—	—	2002	
36	0	0	0	11.2	65.4	23.4	348.2	—	—	—	1554	

续表

Feed No.	Composition, mol%						T, K	Phase boundary, kPa				Reference
	C ₃ H ₈	n-C ₄ H ₁₀	CO ₂	heavy oil	water	DME		L ₁ L ₂ /L ₁ L ₂ V	L ₁ L ₂ V/L ₁ V	L ₁ /L ₁ V	AL ₁ /AL ₁ V	
							363.2	—	—	—	2334	
							378.2	—	—	—	2613	
37	0	0	21.8	59.1	0	19.1	352.25	—	—	3400	—	
							366.45	—	—	3800	—	
							378.05	—	—	4100	—	
							393.35	—	—	4400	—	
38	0	0	19.5	58.2	0	22.3	352.35	—	—	3300	—	
							366.45	—	—	3700	—	
							380.55	—	—	4000	—	
							394.45	—	—	4300	—	
39	0	0	11.5	58.7	0	29.8	352.35	—	—	2300	—	
							366.45	—	—	2700	—	
							378.45	—	—	2900	—	[10]
							393.95	—	—	3100	—	
40	0	0	7.3	21.8	62.6	8.3	351.85	—	—	—	3500	
							366.45	—	—	—	3900	
							378.45	—	—	—	4500	
							393.95	—	—	—	5000	
41	0	0	10.4	20.7	63.7	5.2	352.35	—	—	—	4900	
							366.55	—	—	—	5300	
							378.65	—	—	—	6000	
							390.75	—	—	—	6800	

Table 2 Compositions of solvents/water/heavy oil systems and measured SF at different temperatures

Feed No.	Composition, mol%						T, K	SF	Reference	Feed No.	Composition, mol%						T, K	SF	Reference	
	C ₃ H ₈	n-C ₄ H ₁₀	CO ₂	heavy oil	water	DME					C ₃ H ₈	n-C ₄ H ₁₀	CO ₂	heavy oil	water	DME				
4	67.3	0	0	32.7	0	0	298.55	1.40								362.55	1.18			
							323.95	1.40		22	0	0	28.0	72.0	0	0	323.95	1.05		
							348.35	1.41									348.35	1.05		
							396.15	1.42									362.75	1.08		
5	0	62.0	0	38.0	0	0	298.55	1.34		23	19.6	16.9	34.1	29.4	0	0	296.45	1.41		
							323.95	1.35									317.65	1.43		
							348.35	1.37									327.85	1.43		
							396.15	1.37	[7]	24	16.5	14.2	28.8	40.5	0	0	302.55	1.14	[37]	
6	0	82.5	0	17.5	0	0	298.55	1.99									323.85	1.15		
							323.95	2.03										343.05	1.16	
							348.35	2.07		25	14.7	12.6	25.6	47.1	0	0	322.05	1.09		
							396.15	1.93										342.95	1.09	
7	55.4	15.8	0	28.8	0	0	298.55	1.44									362.85	1.10		
							348.35	1.48		26	12.1	10.4	21.2	56.3	0	0	333.75	1.03		
							396.15	1.50										353.75	1.03	

续表

Feed		Composition, mol%					T, K	SF	Reference	Feed		Composition, mol%					T, K	SF	Reference
No.	C ₃ H ₈	n-C ₄ H ₁₀	CO ₂	heavy oil	water	DME				No.	C ₃ H ₈	n-C ₄ H ₁₀	CO ₂	heavy oil	water	DME			
8	58.5	0	0	41.5	0	0	323.85	1.30							373.35	1.03	[37]		
9	73	0	0	27	0	0	323.85	1.56		32	0	0	0	78.8	0	21.2	348.2	1.0511	
10	81.9	0	0	18.1	0	0	323.85	1.91							363.2	1.0522			
11	58.8	0	0	41.2	0	0	298.85	1.26							378.2	1.0538			
12	65.6	0	0	34.4	0	0	298.85	1.35							393.2	1.0563			
13	74.4	0	0	25.6	0	0	298.85	1.54							408.2	1.0581			
14	67.3	0	0	32.7	0	0	298.85	1.38		33	0	0	0	58.4	0	41.6	348.2	1.1700	
							323.15	1.38							363.2	1.1731			
							348.15	1.40	[88]						378.2	1.1759			
							396.15	1.41							393.2	1.1792	[9]		
15	36.2	0	38.6	25.2	0	0	280.45	1.42							408.2	1.1823			
							298.85	1.47		37	0	0	21.8	59.1	0	19.1	352.25	1.132	
							318.75	1.49							366.45	1.139			
16	0	34.3	31.7	34.0	0	0	298.85	1.37							378.05	1.142			
							318.75	1.37							393.35	1.149			
							347.65	1.38		38	0	0	19.5	58.2	0	22.3	352.35	1.144	
							391.55	1.38							366.45	1.149			
19	25.0	0	25.0	50.0	0	0	298.15	1.14							380.55	1.151	[10]		
							323.15	1.14							394.45	1.154			
							343.15	1.15	[36]	39	0	0	11.5	58.7	0	29.8	352.35	1.159	
							363.15	1.15							366.45	1.162			
							383.15	1.15							378.45	1.168			
21	0	0	54.5	45.5	0	0	323.15	1.15							393.95	1.171			
							343.45	1.15	[37]										

Table 3 Summary of measured and predicted densities for solvents/water/heavy oil/bitumen systems

Solvent	Oil Type	State	Reference	T, K	P, MPa	NPTS ^a	AARD, %		
							VT EOS	IM-E1 ^a	IM-E2 ^b
N ₂	Cold Lake	LV	[16]	304-371	2.5-10.7	12	1.32	—	0.85
N ₂	Athabasca #1	LV	[90]	299-374	1.0-9.8	30	1.46	—	0.72
N ₂	Mackay River	LV	[91]	358-463	2.0-8.0	16	—	—	0.17
CO ₂	Cold Lake	LV	[16]	288-371	2.1-10.9	23	1.56	1.29	0.99
CO ₂	Surmont	LV	[92]	323-462	1.1-6.1	24	0.19	0.25	0.28
CO ₂	Mackay River	LV	[91]	343-463	2.0-8.0	20	—	0.69	0.73
CH ₄	Cold Lake	LV	[16]	299-377	2.6-10.1	16	0.63	0.54	0.49
CO ₂ +CH ₄	Cold Lake	LV	[16]	298-377	2.5-10.5	16	0.98	0.80	0.75
CH ₄	Surmont	LV	[18]	323-463	1.1-8.1	20	0.51	0.28	0.40
CH ₄	Mackay River	LV	[93]	373-463	1.2-4.8	12	0.49	0.48	0.35
CH ₄ +water	Mackay River	ALV	[93]	373-463	1.2-4.8	12	0.87	0.32	0.30
C ₂ H ₆	Cold Lake	LV	[16]	296-375	1.0-10.1	19	0.79	1.22	0.67

续表

Solvent	Oil Type	State	Reference	T , K	P , MPa	NPTS ^a	AARD, %			
							VT EOS	IM-E1 ^a	IM-E2 ^b	
C ₂ H ₆	WC #1	L	[94]	293-423	2.5-10.0	18	0.45	0.35	0.20	
C ₂ H ₆	Surmont	LV	[95]	324-463	1.0-8.2	27	0.76	0.71	0.25	
C ₂ H ₆	Mackay River	LV	[95]	324-464	1.1-8.1	30	0.68	0.45	0.27	
C ₂ H ₆	JACOS	LV	[95]	323-423	1.1-8.2	23	0.98	1.28	0.60	
C ₂ H ₆	Mackay River	LV	[93]	373-463	1.1-4.3	12	0.53	0.78	0.48	
C ₂ H ₆ +water	Mackay River	ALV	[93]	373-463	1.1-4.3	12	0.62	0.30	0.18	
C ₃ H ₈	WC #1	L	[94]	293-448	2.5-10.0	40	1.78	1.04	0.68	
C ₃ H ₈	Surmont	LV	[24]	323-463	1.1-8.1	17	1.36	0.35	0.41	
C ₃ H ₈	Mackay River	LV	[93]	373-463	1.2-4.4	12	1.49	0.65	0.67	
C ₃ H ₈ +water	Mackay River	ALV	[93]	373-463	1.2-4.4	12	1.23	0.56	0.67	
Water	Mackay River	AL	[93]	373-463	3.0	4	0.45	—	0.32	
<i>n</i> -C ₄ H ₁₀	WC #1	L	[94]	293-448	2.5-10.0	28	—	1.28	0.99	
<i>n</i> -C ₄ H ₁₀	Surmont	LV	[94]	373-463	0.8-5.0	16	2.52	1.00	1.16	
<i>n</i> -C ₅ H ₁₂	Athabasca #2	L	[96]	323-483	1.0-1.0	21	—	0.34	0.28	
<i>n</i> -C ₅ H ₁₂	Surmont	LV	[92]	374-423	0.5-1.5	6	1.72	0.92	1.05	
<i>n</i> -C ₅ H ₁₂	Surmont	L	[97]	323-464	2.0-10.0	116	—	0.52	0.54	
<i>n</i> -C ₅ H ₁₂	WC #1	L	[94]	293-448	0.1-10.0	54	—	1.20	0.80	
<i>n</i> -C ₆ H ₁₄	Surmont	L	[98]	296-463	2.0-10.1	150	—	0.30	0.28	
<i>n</i> -C ₆ H ₁₄	Mackay River	L	[99]	294-459	2.0-10.0	78	—	2.34	2.29	
<i>n</i> -C ₆ H ₁₄	Athabasca #3	L	[28]	328-447	1.5-6.6	30	—	0.20	0.18	
cyclohexane	WC #2	L	[94]	294-448	0.1-10.0	62	—	—	0.47	
<i>n</i> -C ₇ H ₁₆ + toluene	WC #1	L	[94]	294-448	0.1-10.0	94	—	—	0.78	
<i>n</i> -C ₇ H ₁₆	Surmont	L	[25]	295-463	2.0-10.0	145	—	0.62	0.30	
toluene	Athabasca #4	LV	[19]	371-593	0.1-3.6	12	7.56	—	0.02	
Toluene + water	Athabasca #4	ALV	[19]	452-574	1.7-12.5	13	14.67	—	1.38	
toluene	WC #1	L	[94]	293-448	0.1-10.0	95	—	—	0.45	
toluene	Surmont	L	[17]	294-463	2.0-10.0	200	—	—	0.51	
DME	Surmont	LV	[100]	373-423	1.1-6.1	13	1.18	—	0.54	
DME	Athabasca #3	L	[28]	328-446	2.0-7.0	46	—	—	0.47	
—	—	—	—	—	—	Overall	1649	1.98	1.05	0.73

Note : NPTS^a denotes the number of experimental data points. IM-E1^a denotes ideal mixing rule with effective density calculated using the equation of Saryazdi^[99] or Saryazdi et al.^[100] IM-E2^b denotes ideal mixing rule with effective density calculated using the equation of Chen and Yang^[40]

Table 4 Summary of measured and predicted viscosities for solvents/water/heavy oil/bitumen systems

Heavy oil/ bitumen	Solvent	Equilibria type	Reference	T , K	P , MPa	Viscosity, mPa·s	NPTS ^a	Power-law				
								n (weight- based)	AARD, % (weight- based)	n (volume- based)	AARD, % (volume- based)	AARD, % (Cragoe)
Surmont	Methane	L ₁ V	[18]	323.1-463.4	1.09-8.10	9.2-11900.0	20	-0.300	14.8	-0.182	11.6	53.0
bitumen	Propane	L ₁ V	[24]	323.4-462.9	1.08-8.12	1.93-71.70	17	-0.261	12.1	-0.121	22.9	12.9
	<i>n</i> -butane	L ₁ V	[26]	373.3-463.0	0.83-5.00	1.54-17.00	16	-0.282	22.5	-0.134	19.4	23.5
	<i>n</i> -pentane	L ₁ V	[92]	422.3-422.6	0.46-1.49	1.73-6.68	4	-0.199	14.0	-0.070	15.7	52.5

续表

Heavy oil/ bitumen	Solvent	Equilibria type	Reference	<i>T</i> , K	<i>P</i> , MPa	Viscosity, mPa·s	NPTS ^a	Power-law				
								<i>n</i> (weight- based)	AARD, % (weight- based)	<i>n</i> (volume- based)	AARD, % (volume- based)	AARD, % (Cragoe)
Mackay River bitumen	CO ₂	L ₁ V	[92]	323.2-462.9	1.06-6.13	8.32-3663.00	24	-0.222	13.4	-0.198	16.8	21.6
	Methane	L ₁ V	[93]	373.2-463.2	1.17-4.76	8.5-167.7	12	-0.369	8.7	-0.178	9.5	17.8
	Methane	AL ₁ V	[93]	373.2-463.3	1.17-4.76	7.7-154.0	12	-0.369	9.0	-0.178	10.1	17.7
	Ethane	L ₁ V	[93]	373.2-463.3	1.14-4.28	6.6-146.2	12	-0.299	11.1	-0.149	16.2	21.4
	Ethane	AL ₁ V	[93]	373.2-463.3	1.14-4.28	6.0-132.7	12	-0.299	7.4	-0.149	11.2	19.5
	Propane	L ₁ V	[93]	373.2-463.3	1.17-4.38	2.1-70.4	12	-0.275	13.8	-0.111	9.1	10.4
	Propane	AL ₁ V	[93]	373.2-463.3	1.17-4.38	2.1-81.0	12	-0.275	14.8	-0.111	4.9	11.3
	<i>n</i> -butane	L ₁ V	[93]	373.2-453.3	0.88-4.21	0.7-9.8	10	-0.291	35.1	-0.181	37.5	37.5
	<i>n</i> -butane	AL ₁ V	[93]	373.2-453.3	0.88-4.21	1.4-13.5	10	-0.291	30.6	-0.181	34.9	33.6
Senlac heavy oil	Water	AL ₁	[93]	373.2-463.2	3.0	11-254.9	4	—	—	—	—	—
	Methane	L ₁ V	[101]	298.2-423.2	5.0	5.14-566.00	3	-0.345	30.4	-0.218	17.5	82.1
	Methane	AL ₁ V	[101]	298.2-423.2	5.0	5.00-555.00	3	-0.345	20.5	-0.218	8.2	71.9
	CO ₂	L ₁ V	[101]	298.2-423.2	5.0	4.31-74.60	3	-0.215	23.6	-0.206	14.4	19.0
	CO ₂	AL ₁ V	[101]	298.2-353.2	5.0	19.4-70.0	2	-0.215	23.6	-0.206	8.9	10.6
Cold Lake bitumen	Methane	L ₁ V	[101]	299.8-377.0	2.57-10.08	47-15000	16	-0.316	31.8	-0.172	14.6	89.1
	Ethane	L ₁ V	[101]	296.1-375.9	1.02-10.07	8.6-3800.0	19	-0.254	24.4	-0.121	15.9	37.1
	N ₂	L ₁ V	[101]	303.9-371.4	2.46-10.66	104-16300	12	-0.244	16.7	—	—	17.1
	CO ₂	L ₁ V	[101]	287.9-371.4	2.06-10.94	26-7400	23	-0.189	21.2	-0.178	12.8	25.1
Overall							258		19.0		15.5	32.6

Table 5 Summary of the experimentally measured solubilities and AARDs^[102-112]

Hydrocarbons	<i>T</i> , K	<i>X</i> _{HC}	<i>X</i> _w	NPTS ^a	AARD, %	
					Aqueous phase	Oleic phase
Propane	285.3-422.0	2.0×10 ⁻⁴ -3.7×10 ⁻⁴	1.4×10 ⁻⁴ -7.6×10 ⁻³	9	10.23	36.90
<i>n</i> -butane	310.9-477.6	6.6×10 ⁻⁵ -7.4×10 ⁻⁴	5.0×10 ⁻⁴ -1.1×10 ⁻¹	6	30.29	24.70
<i>n</i> -pentane	273.2-410.5	1.1×10 ⁻⁵ -4.8×10 ⁻⁵	1.8×10 ⁻⁴ -6.3×10 ⁻⁴	18	37.83	5.63
<i>n</i> -hexane	273.2-473.2	2.4×10 ⁻⁶ -2.2×10 ⁻⁵	1.9×10 ⁻⁴ -1.7×10 ⁻¹	34	24.00	6.84
<i>n</i> -heptane	273.2-460.2	5.2×10 ⁻⁷ -2.6×10 ⁻⁵	1.9×10 ⁻⁴ -1.7×10 ⁻³	24	4.62	4.57
<i>n</i> -octane	273.2-479.5	1.0×10 ⁻⁷ -2.3×10 ⁻⁵	2.0×10 ⁻⁴ -1.3×10 ⁻³	22	23.10	7.67
<i>n</i> -nonane	288.2-409.8	1.9×10 ⁻⁸ -2.9×10 ⁻⁷	6.2×10 ⁻⁴ -7.5×10 ⁻⁴	8	26.65	2.92
<i>n</i> -decane	293.2-475.2	3.3×10 ⁻⁹ -2.6×10 ⁻⁶	5.1×10 ⁻⁴ -9.8×10 ⁻²	7	54.74	6.60
<i>n</i> -dodecane	298.2-313.2	3.6×10 ⁻¹⁰ -3.6×10 ⁻¹⁰	7.5×10 ⁻⁴ -1.4×10 ⁻³	2	30.59	5.33
<i>n</i> -tetradecane	298.0-298.0	2.4×10 ⁻¹⁰ -2.4×10 ⁻¹⁰	—	1	61.93	—
<i>n</i> -hexadecane	293.0-313.0	1.8×10 ⁻¹⁰ -1.8×10 ⁻¹⁰	1.1×10 ⁻³ -3.6×10 ⁻³	5	79.33	14.80
<i>n</i> -eicosane	298.0-298.0	1.4×10 ⁻¹⁰ -1.4×10 ⁻¹⁰	—	1	67.66	—
Overall					26.69	9.09

Table 6 Summary of the experimental database of mass transfer

Feed No.	Composition, mol%				Initial pressure, kPa	T, K	Reference
	CO ₂	C ₃ H ₈	n-C ₄ H ₁₀	heavy oil			
42	74.05	0	0	25.95	3741		
43	60.94	11.28	0	27.78	3799	294.55	[114]
44	35.67	0	4.71	59.62	1128		
45	70.88	0	0	29.12		298.55	
46	73.94	0	0	26.06	5400	317.65	[115]
47	67.35	0	0	32.65		336.65	
48	78.21	0	0	21.79		330.95	
49	62.91	15.97	0	21.12	5500	331.15	[116]
50	48.61	26.28	0	25.11		329.25	
51	0.00	0	30.71	69.29	5400	329.65	
52	65.86	0	7.09	27.05	5520	329.15	[117]
53	61.32	10.57	4.24	23.87	5540	329.25	

Table 7 Comparison of molecular diffusion coefficients in different oils

Gas system	Crude oil	Viscosity, cP	P, kPa	T, K	Diffusion coefficient, 10 ⁻¹⁰ m ² /s	Reference	
CO ₂			3741-3371	294.55	4.30	[114]	
				298.55	6.17	[115]	
	Lloydminster heavy oil	12854@294.55 K	5400	317.65	14.97	[117]	
				336.65	21.01	[115]	
	Athabasca bitumen	361700@293.15 K	5000	323.15	5.00	[118]	
				348.15	7.10		
				4000	323.15	2.20-3.10	
	Athabasca bitumen (SYN)	821000@298.15 K		348.15	3.40-4.90		
				8000	323.15	3.60-5.20	
				348.15	6.90-8.90	[119]	
				4000	323.15	2.20-3.30	
	Athabasca bitumen(SCF)	224500@298.15 K		348.15	3.51-5.02		
				8000	323.15	5.42-7.28	
	Athabasca bitumen	100000 @323.15 K		3805	323.15	3.60	[120]
	Athabasca bitumen	~ 2000000@294 K		3100-5600	294.15	1.20-2.40	[121]
	Lloydminster heavy oil	12854@294.55 K		5500	330.95	21.00	[116]
	Lloydminster heavy oil	20267@297.05 K		3500-4200	297.05	4.60-5.30	[122]
				3000		2.30	
	Lloydminster heavy oil	23000@297.05 K		4000	297.05	2.80	
				5000		3.20	[123]
			6000		5.50		
Lloydminster heavy oil	12854@294.55 K		3950	293.85	5.54	[124]	
Lloydminster heavy oil	13,924@294.55 K		3945	293.85	5.55 (CO ₂) 7.48 (C ₃ H ₈)	[125]	
Lloydminster heavy oil	7176@299.65 K		855-817	299.65	4.26*	[126]	
Lloydminster heavy oil	7176@299.65 K		854-783	299.65	4.06* (CO ₂) 16.63* (C ₃ H ₈)	[126]	

续表

Gas system	Crude oil	Viscosity, cP	P , kPa	T , K	Diffusion coefficient, 10^{-10} m ² /s	Reference
C_3H_8	Lloydminster heavy oil	23000@297.05 K	400-900	297.05	0.90-6.80	[123]
	Lloydminster heavy oil	20267@297.05 K	500-730	297.05	7.90-11.00	[122]
	Lloydminster heavy oil	24137@297.05 K	200-800	297.05	0.53-4.90	[127]
	Lloydminster heavy oil	13144@290 K	400-600	298.00	2.12-3.59	[128]
	MacKay bitumen	127868@297.05 K	413.7 827.4	297.15	0.26 4.17	[129]
	Cactus Lake heavy oil	724.15@299 K	400-600	303.00	6.95-8.93	[130]
$n-C_4H_{10}$	Lloydminster heavy oil	13144@290 K	100-150	298.00	1.10-1.84	[128]
$n-C_4H_{10}$	Lloydminster heavy oil	12854@294.55 K	529	329.65	7.01	[116]
70 mol% CO_2 30 mol% C_3H_8	Lloydminster heavy oil	23000@297.05 K	1003-3005	297.05	0.82-8.20	[123]
84.38 mol% CO_2 15.62 mol% C_3H_8	Lloydminster heavy oil	12854@294.55 K	3799-3349	294.55	1.05 (CO_2) 13.70 (C_3H_8)	[114]
					3.77**	
88.33 mol% CO_2 11.67 mol% $n-C_4H_{10}$	Lloydminster heavy oil	12854@294.55 K	1128-982	294.55	4.06 (CO_2) 13.34 (C_3H_8)	[114]
					4.63**	
79.75 mol% CO_2 20.25 mol% C_3H_8	Lloydminster heavy oil	12854@294.55 K	5500	331.15	1.01 (CO_2) 15.30 ($n-C_4H_{10}$)	[114]
					4.90**	
64.90 mol% CO_2 35.10 mol% C_3H_8	Lloydminster heavy oil	12854@294.55 K	5500	329.25	1.92 (CO_2) 13.41 ($n-C_4H_{10}$)	[114]
					2.88**	
90.29 mol% CO_2 9.71 mol% $n-C_4H_{10}$	Lloydminster heavy oil	12854@294.55 K	5520	329.15	10.00 (CO_2) 14.40 (C_3H_8)	[116]
					11.99**	
80.55 mol% CO_2 13.88 mol% C_3H_8 5.57 mol% $n-C_4H_{10}$	Lloydminster heavy oil	12854@294.55 K	5540	329.25	9.36 (CO_2) 22.37 (C_3H_8)	[131]
					16.30**	
80.55 mol% CO_2 13.88 mol% C_3H_8 5.57 mol% $n-C_4H_{10}$	Lloydminster heavy oil	12854@294.55 K	5540	329.25	19.50 (CO_2) 27.50 ($n-C_4H_{10}$)	[117]
					23.80**	
80.55 mol% CO_2 13.88 mol% C_3H_8 5.57 mol% $n-C_4H_{10}$	Lloydminster heavy oil	12854@294.55 K	5540	329.25	7.02 (CO_2) 26.53 (C_3H_8) 29.04 ($n-C_4H_{10}$)	[117]
					14.78**	

*Note: porous medium is involved **Note: Apparent diffusion coefficient of gas mixture

Table 8 Compositions of nonequilibrium CCE experiments at constant volume expansion rate^[132]

Feed No.	Composition, mol%				T , K	P_b , kPa	P_{pb} , kPa	P_s , kPa	Expansion volume rate, cm ³ /hr	Rebound pressure, kPa
	CH_4	CO_2	C_3H_8	heavy oil						
54	0	27.7	0	72.3	303.3	2172	1413	758	0.3	110
					323.5	2661	2055	607	0.3	28
					342.8	3351	2682	669	0.3	0
55	0	19.7	28.7	51.6	303.3	2220	1558	662	1.5	69
					323.5	2972	2103	869	1.5	193
					342.8	4054	3696	359	1.5	34
					342.8	4054	3971	83	0.8	21
56	14.4	0	0	85.6	342.8	4061	3061	1000	0.2	0
					342.8	4061	2717	1344	0.4	0
					342.8	4061	2392	1669	0.8	0

Table 9 Compositions of nonequilibrium CCE experiments with constant pressure decline rate^[133-135]

Feed No.	Composition, mol%				T, K	P_b, kPa	P_{pb}, kPa	P_s, kPa	Pressure decline rate, kPa/min	Average gas exsolution rate, 10^{-6} mol/kPa	$\frac{P_{pb} - P_b}{P_{pb}}$
	CH ₄	CO ₂	C ₃ H ₈	heavy oil							
57	0	30.4	0	69.6	303.3	2250	2100	150	12	0.852	0.40
					303.3	2250	1200	1050	20	1.423	0.41
					323.4	2750	2150	600	20	0.756	0.26
58	8.8	0	29.0	62.2	323.4	2900	2500	400	20	2.156	0.32
					342.7	5000	4700	300	20	1.298	0.06
59	8.8	14.1	0	77.1	342.7	4978	3516	1462	20	2.298	0.64

3 Theoretical Improvements

Because of its good accuracy and simplicity in the petrochemical industry, the PR EOS has been one of the most successfully applied models for calculating thermodynamic properties of pure substances and their mixtures^[43,137]. Modifications have been made to improve accuracy and performance of the PR EOS. The improvements have been grouped into four main categories: (1) alpha function; (2) acentric factor; (3) BIP; and (4) mixing rules, allowing the PR EOS to be more applicable to complex conditions with good and consistent accuracy.

3.1 Alpha Function

Numerous studies have been performed to modify alpha function to improve the prediction of vapour pressure for a pure substance^[137]. There are two basic forms of alpha functions, i. e., the Soave-type^[44] and the logarithm-type^[57]. These two types of alpha functions have limits, including one of which is only applicable to light to medium hydrocarbons^[138].

Based on the vapour pressure database of 59 non-hydrocarbons and hydrocarbons, including heavy alkanes up to *n*-tritetracontane (*n*-C₄₃H₈₈), the recently improved alpha function developed by Li and Yang^[49], which combines the characteristics of both the Soave-type and the logarithm-type function, leads to more accurate calculation of vapour pressures for the 59 chemical species and 1165 data points with an average absolute relative deviation (AARD) of 1.90% and a maximum absolute relative deviation (MARD) of 21.22%. It is reported that the newly developed alpha function leads to the best prediction of the vaporization enthalpy with an AARD of 3.92%

compared with the other existing alpha functions evaluated^[49]. Later on, such a modified alpha function has been applied to accurately predict phase behaviour and physical properties not only for light hydrocarbons and non-hydrocarbon substances, but also for heavy hydrocarbons by treating heavy oil as single PC^[7,21,88,124-126] and multiple PCs^[9-10,36-37,115,117,132,139-140].

The Soave-type alpha function used in the original PR EOS is expressed as,

$$\alpha = [1 + (0.37464 + 1.54226\omega - 0.2699\omega^2)(1 - T_r^{0.5})]^2 \quad (1a)$$

where α is the alpha function, T_r is the reduced temperature, and ω is the acentric factor.

The newly modified alpha function with an acentric factor defined at $T_r = 0.7$ is formulated as follows^[49],

$$\alpha(T_r, \omega) = \exp \left\{ \begin{aligned} & \left(\frac{0.13280 - 0.05052\omega +}{0.25948\omega^2} \right) (1 - T_r) \\ & + 0.81769 \ln \left[\frac{1 + \left(\frac{0.31355 + 1.86745\omega -}{0.52604\omega^2} \right)^2}{(1 - \sqrt{T_r})} \right] \end{aligned} \right\} \quad (1b)$$

Another newly modified alpha function with an acentric factor defined at $T_r = 0.6$ is formulated as follows^[49],

$$\alpha(T_r, \omega) = \exp \left\{ \begin{aligned} & \left(\frac{0.34580 - 0.59700\omega +}{0.27040\omega^2} \right) (1 - T_r) \\ & + 0.92030 \ln \left[\frac{1 + \left(\frac{-0.53261 + 1.75415\omega -}{0.40127\omega^2} \right)^2}{(1 - \sqrt{T_r})} \right] \end{aligned} \right\} \quad (1c)$$

It is interesting to note that Eq. 1c yields much better prediction accuracy of vapour pressures of polar or nonpolar non-hydrocarbon compounds, light hydrocarbons and heavy hydrocarbons than those of

Eq. 1b.

Subsequently, Chen and Yang^[69] expanded vapour pressure database to 1880 data points and proposed a new alpha function with an acentric factor defined at $T_r = 0.6$, i.e.,

$$\alpha = \exp \left\{ \begin{array}{l} (0.33730 - 0.26346\omega^2 + 0.05297\omega^2)(1 - T_r) \\ + 1.01711 \ln \left[1 + \frac{(-0.42587 + 1.16423\omega - 0.10857\omega^2)}{(1 - \sqrt{T_r})} \right]^2 \end{array} \right\} \quad (1d)$$

As pointed by Peng and Robinson, a modified alpha function which can accurately reproduce the water vapour pressure is able to significantly improve the calculation accuracy of phase equilibrium for aqueous phase^[36]. As for water-involved mixtures, a new alpha function for water compound is modified by improving its prediction for water vapor pressure in a temperature range of 273.16-647.10 K with an overall AARD of 0.07%, while it is formulated as follows^[22],

$$\alpha_{H_2O} = [c_1 + c_2(1 - T_{rw}) - c_3(1 - T_{rw}^{-1}) + c_4(1 - T_{rw}^{-2})]^2 \quad (2)$$

where T_{rw} is the reduced temperature of water, $c_1 = 1.00095$, $c_2 = 0.39222$, $c_3 = 0.07294$, and $c_4 = 0.00706$, respectively.

It is found that the newly modified alpha function is able to predict the CO₂ solubility in water with an overall AARD of 6.12%^[22]. Also, such obtained alpha functions together with four volume translation (VT) strategies have been comparatively evaluated with different heavy oils saturated with the aforementioned solvents, showing excellent performance in predicting their saturation pressures^[139] and densities^[140] by treating heavy oil/bitumen as one PC and multiple PCs, respectively.

3.2 Acentric Factor

The acentric factor, which reflects the deviation of acentricity or non-sphericity of a compound molecule from that of a simple fluid, imposes a significant impact on the alpha function in the PR EOS. The acentric factor originally developed by Pitzer and defined at a reduced temperature of 0.7 is formulated as follows^[62],

$$\omega = -\log(P_r)_{T_r=0.7} - 1 \quad (3a)$$

It is found that the generalized correlation of acentric factor proposed by Pitzer defined at a reduced temperature of 0.7 is able to accurately predict the vapour pressures at reduced temperatures between 0.7 and 1.0; however, it is less accurate in representing the characteristics of heavy hydrocarbons when a temperature is much lower than 70% of its critical temperature^[49]. To balance the characterization of both light and heavy hydrocarbons, the acentric factor has been redefined at a reduced temperature of 0.6 instead of 0.7 as initially defined by Pitzer^[62], which is expressed as^[49],

$$\omega' = -\log(P_r)_{T_r=0.6} - 1 \quad (3b)$$

Compared to the evaluated alpha functions used for the PR-EOS, it is found that the newly developed alpha function (i.e., Eq. 1b) with the redefined acentric factor (i.e., Eq. 3b) yields a much better prediction of vapor pressures for the 59 pure substances^[49].

3.3 BIP

For solvent/heavy oil pairs, the BIPs are usually obtained by tuning then to match the experimentally measured saturation pressures or solvent solubilities in heavy oil for the solvent-heavy oil mixtures^[88]. Specifically, the solubility data of CO₂/heavy oil, C₃H₈/heavy oil, and *n*-C₄H₁₀/heavy oil are used to develop the BIP correlations for further calculation of phase behaviour and physical properties of petroleum fluids. The BIP correlations of the solvent-heavy oil pair developed by Li et al.^[21] are respectively expressed by,

$$\delta_{14} = -0.4560T/T_{co} + 0.1817 \quad (4a)$$

$$\delta_{24} = -0.2331T/T_{co} + 0.1198 \quad (4b)$$

$$\delta_{34} = -0.5462T/T_{co} - 0.4596SG_o - 0.0238\omega_o + 0.7523 \quad (4c)$$

where δ_{14} , δ_{24} , and δ_{34} are the BIPs between C₃H₈ and heavy oil, *n*-C₄H₁₀ and heavy oil, CO₂ and heavy oil, respectively, T_{co} , SG_o , and ω_o are the critical temperature, specific gravity, and acentric factor of the Lloydminster heavy oil, respectively.

Li and Yang^[22] developed a new polynomial temperature-dependent BIP correlation between CO₂ and water in the presence and absence of hydrocarbons by matching CO₂ solubility in water in a temperature range of 273.15 to 448.15 K and pressure as high as 100 MPa. Their new polynomial BIP correla-

tion is provided as follows,

$$\delta_{CO_2, \text{modified}}^{A0} = -1.104324 + 2.040527T_r - 1.417707T_r^2 + 0.379003T_r^3 \quad (5)$$

3.4 Mixing Rule

Mixing rules are introduced to extend the application of the EOSs to mixtures. As for mixtures containing polar components, the classical mixing rules are limited to predict the mixture properties because they are inappropriate to represent the hydrogen bonds and polar interactions^[141-142]. The Huron-Vidal mixing rule is non-classical one, which is widely used because it yields better prediction of the phase behaviour and mutual solubility between water and solvents in comparison with the classical mixing rule^[30-31, 143]. Furthermore, the Huron-Vidal mixing rule only has few unknown parameters, while it can be reduced to the classical mixing rule, which is considered as one of the significant advantages.

The parameter a for the Huron-Vidal mixing rule is defined as^[74, 143],

$$a = b \left[\sum_{i=1}^{N_c} y_i \left(\frac{a_i}{b_i} \right) + \frac{G_\infty^E}{\lambda} \right] \quad (6)$$

where λ is an EOS-dependent parameter, and G_∞^E is the excess Gibbs free energy at infinite pressure, which are provided as follows^[143],

$$\lambda = \frac{1}{2\sqrt{2}} \ln \left(\frac{\sqrt{2} + 1}{\sqrt{2} - 1} \right) \quad (7)$$

$$\frac{G_\infty^E}{RT} = \frac{\sum_{i=1}^{N_c} y_i \sum_{j=1}^{N_c} y_j b_j \tau_{ji} \exp(-\alpha_{ji} \tau_{ji})}{\sum_{k=1}^{N_c} y_k b_k \exp(-\alpha_{ki} \tau_{ki})} \quad (8)$$

where α_{ji} is the interaction parameter, $\alpha_{ii} = 0$, $\alpha_{ij} = \alpha_{ji}$, and the parameter τ_{ji} for the Huron-Vidal mixing rule is expressed as,

$$\tau_{ji} = \frac{g_{ji} - g_{ii}}{RT} \quad (9)$$

where g_{ji} is the energy parameter, J/mol, while g_{ji} and g_{ij} as a function of temperature are provided as follows^[142],

$$g_{ij} - g_{ji} = (g_{ij}^I - g_{ji}^I) + T(g_{ij}^{II} - g_{ji}^{II}) \quad (10a)$$

$$g_{ji} - g_{ii} = (g_{ji}^I - g_{ii}^I) + T(g_{ji}^{II} - g_{ii}^{II}) \quad (10b)$$

It is important to note that the Huron-Vidal mixing rule can apply to both polar and non-polar substances, while it can be simplified as the classical

mixing rule when polar substances are not present in a mixture.

4 Results and Discussion

4.1 Phase Boundary

CO₂/heavy oil system. Li et al.^[144] applied the VT PR EOS together with the modified alpha function to determine saturation pressures for binary CO₂-heavy oil systems, while the details are tabulated in Table 1. Figure 1 presents the measured and predicted saturation pressures for the aforementioned systems (i.e., Feeds #21 and #22). It can be observed that the saturation pressure increases with temperature for a given feed, indicating that at a specific reservoir pressure, the solubility of CO₂ in heavy oil at a lower temperature is larger than that at a higher temperature. As for applying the modified PR EOS by Li et al.^[88] together with the characterized six PCs of heavy oil and new improved BIP correlation for binary CO₂-heavy oil systems, Feeds #21 and #22 have a generally good agreement between the measured and calculated ones, which can be observed in Figure 1 with an overall AARD of 4.6%^[37].

C₃H₈/heavy oil system. Figure 2 compares the measured saturation pressures and their predicted ones for the C₃H₈-heavy oil system (see Feeds #8-#13 in Table 1) at the temperature of 298.85 and 323.85K, respectively. As can be seen, the saturation pressure increases with an increase of the mole percentage of C₃H₈ at the same temperature, whereas it increases with temperature for a C₃H₈-heavy oil mixture. Overall, the PR EOS model with the modified

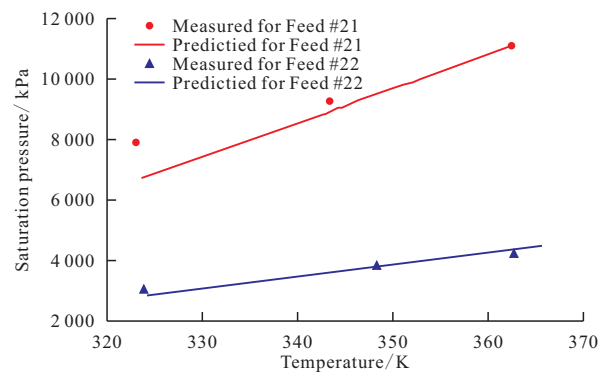


Figure 1 Comparison of the measured saturation pressures of CO₂/heavy oil systems and the predicted ones (Modified from [37]).

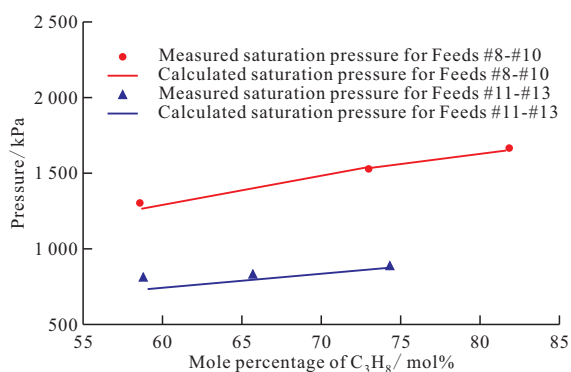


Figure 2 Comparison of the measured and calculated saturation pressures for binary C_3H_8 /heavy oil system with Feeds #8-#10 at 323.85 K and with Feeds #11-#13 at 298.85 K, respectively (Modified from [142])

alpha function is able to accurately predict the saturation pressure with an AARD of 2.82% for the experimental data points in Figure 2^[88].

$n-C_4H_{10}$ /heavy oil system. Figure 3 compares the measured and calculated saturation pressures for the $n-C_4H_{10}$ /heavy oil systems (see Feeds #5 and #6 in Table 1). It can be found from Figure 3 that the measured and calculated saturation pressures match well, although the accuracy is reduced at temperatures close to the critical temperature of $n-C_4H_{10}$. As for the deviation near the critical temperature, it might be because the PR EOS model is less accurate when used for modelling $n-C_4H_{10}$ /heavy-oil phase behaviour at temperatures close to the critical temperature of $n-C_4H_{10}$ ^[21].

$C_3H_8/n-C_4H_{10}/CO_2$ /heavy oil system. The PR EOS incorporated with the modified alpha function is used to quantify the phase behaviour of the quaternary systems by characterizing heavy oil as six PCs^[37,145]. The measured saturation pressures for each of four quaternary feeds are presented in Table 1. The

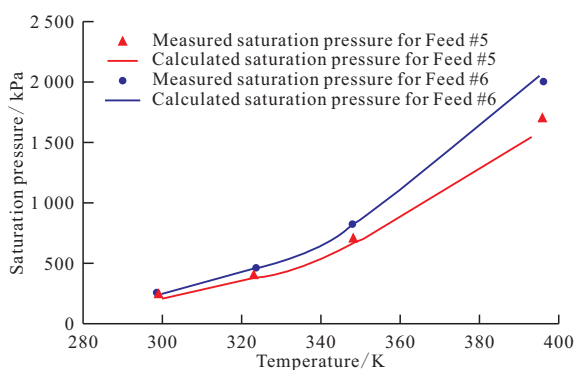


Figure 3 Comparison of the measured and predicted saturation pressures for binary $n-C_4H_{10}$ -heavy oil system with Feed #5 and Feed #6 (Modified from [7])

AARD for predicting the twelve measured saturation pressures of quaternary systems (i.e., Feeds #23-#26) by using such BIP matrix is computed to be 27.3%, implying that the prediction accuracy for quaternary systems shall be further improved by performing the tuning process.

The measured and predicted saturation pressures of Feeds #23-#26 at a temperature range of 296.45-373.35K are plotted in Figure 4. The predicted saturation pressures agree well with the measured data, resulting in AARDs of 3.8%, 7.6%, 7.5%, and 7.7%, respectively. Each AARD is less than 10%, proving that the PR EOS incorporated with modified alpha function can accurately predict the phase behaviour of the aforementioned system.

C_3H_8/CO_2 /water/heavy oil system. Figure 5 depicts the measured and calculated phase boundary pressures of C_3H_8/CO_2 /water/heavy oil systems. As can be seen, the experimentally measured and theoretically calculated three-phase AL_1V boundary pressures match quite well with each other, illustrating the newly developed isenthalpic flash algorithm is accurate in describing phase boundaries of the aforementioned systems^[36,146]. Also, it is found that the phase boundary pressure is reduced with an increase of water content in the aforementioned systems.

DME/heavy oil system. The tuned BIP_{DME-HO} ^[10] is used to regenerate the experimentally measured saturation pressures of Feeds #32 and #33 for the two DME/heavy oil mixtures with the corresponding comparison of the calculated and measured saturation pressures. Good agreements can be found from the root mean square relative error (RMSRE) within

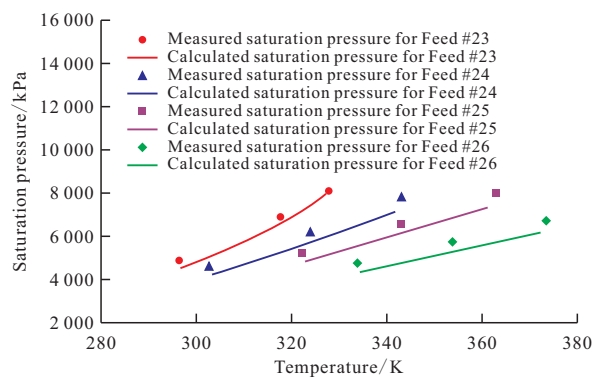


Figure 4 Comparison of the measured and predicted saturation pressures for quaternary $C_3H_8/n-C_4H_{10}/CO_2$ /heavy oil systems with Feeds #23-#26 (Modified from [37]).

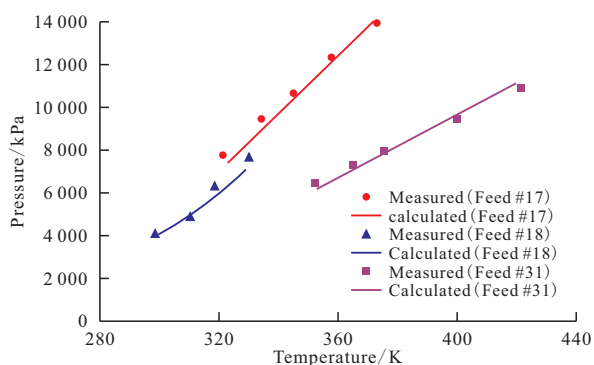


Figure 5 Comparison of the measured and predicted saturation pressures for quaternary $C_3H_8/CO_2/water/heavy$ oil systems with Feeds #17, #18, and #31 (Modified from [36, 146]).

2.88% for a total of 10 data points, indicating that the developed thermodynamic model is able to accurately calculate the saturation pressures for DME-heavy oil systems.

DME/water/heavy oil system. Non-classical mixing rules are commonly needed to describe phase behaviour and physical properties of petroleum fluids containing polar components. The experimentally measured saturation pressures for Feeds #34 through #36 are listed in Table 1. Huang et al. [10] compared the experimentally measured and theoretically calculated saturation pressures for the aforementioned mixtures by implementing the PR EOS associated with the van der Waals and Huron-Vidal mixing rules, respectively. Similar to the DME/heavy oil mixtures, it is found that the saturation pressures of DME/water/heavy oil mixtures increase with temperature, indicating that the amount of DME dissolved in the oleic phase is reduced with an increment of temperature. Comparing the saturation pressures of Feed #34 with those of Feed #33, it can be observed that adding water to the DME/heavy oil mixture leads to an increase in saturation pressure. This is because water molecules evaporate into the vapour phase at high-temperature and low-pressure conditions [74]. It can also be found that the system saturation pressures increase with the DME concentration in the mixture. In addition, a good agreement is observed between the measured saturation pressures and calculated ones obtained by the Huron-Vidal mixing rule (overall RMSRE: 5.08%), while there exist large deviations for the van der Waals mixing rule (overall RMSRE:

17.87%), implying that the PR EOS and the non-classical mixing rule can reproduce the saturation pressures with an acceptable accuracy for the DME/water/heavy-oil mixtures. The details of the comparison of these three mixing rules can be found elsewhere [9].

DME/CO₂/heavy oil system. Figure 6 shows the experimentally measured and theoretically calculated saturation pressures of DME/CO₂/heavy oil mixtures. It should be mentioned that the tuned BIP between DME and heavy oil is 0.013, while the BIP between CO₂ and DME is from the literature [147]. It can be seen that the calculated saturation pressures match quite well with the measured ones, indicating that the developed model can be used to predict the saturation pressures for DME/CO₂/heavy oil mixtures.

DME/CO₂/water/heavy oil system. Figure 7 plots the comparison of the measured and calculated saturation pressures of DME/CO₂/water/heavy oil mixtures by applying the van der Waals and Huron-

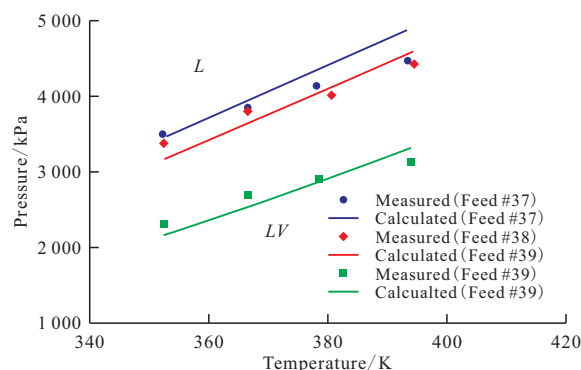


Figure 6 Comparison of the measured saturation pressures of DME/CO₂/heavy oil systems and the predicted ones by using the modified PR EOS (Modified from [147]).

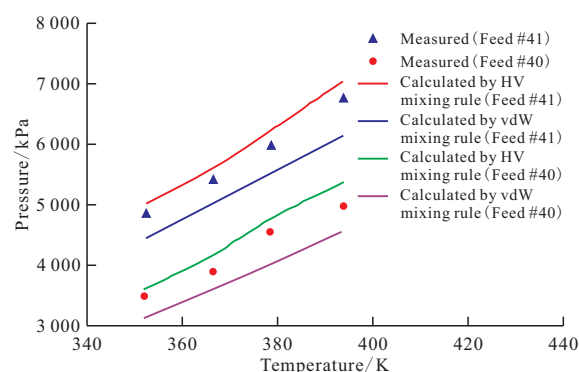


Figure 7 Comparison of the measured saturation pressures of DME/CO₂/water/heavy oil systems and the predicted ones by using the PR EOS incorporated with the van der Waals (vdW) and Huron-Vidal (HV) mixing rules, respectively (Modified from [147]).

Vidal mixing rules, respectively. As can be seen, the predicted results obtained from the Huron-Vidal mixing rule are much better than those from the van der Waals mixing rule. As for the two feeds (i.e., Feeds # 39 and #40), the overall RMSRE obtained from the Huron-Vidal mixing rule is 4.90%, compared to 8.59% obtained from the van der Waals mixing rule^[147].

4.2 SFs

Because SF is an essential parameter in simulating and optimizing heavy-oil-recovery processes involving solvent utilization, its measurement and prediction is of important significance^[88].

CO₂/heavy oil system. As for the swelling factor for CO₂-heavy oil systems, it is found that the SFs are insensitive to temperature but mainly influenced by the CO₂ concentration in a given system. The PR EOS with and without the volume shift is applied in each characterization scheme (i.e., Feeds #21 and #22 in Table 1)^[37,144], while the measured swelling factors can be found in Table 2. For the scheme of treating heavy oil as a single PC, the AARD for the predicted swelling factor can be improved from 2.71% (without volume shift) to 1.88% (with volume shift). For the scheme of treating heavy oil as six PCs, both scenarios can accurately predict the swelling factor with the AARDs of 1.79% (without volume shift) and 1.39% (with volume shift), respectively. In summary, the volume translated PR EOS coupled with the six PCs of heavy oil is the most reliable model to reproduce the phase and volumetric behaviour of CO₂-heavy oil systems.

C₃H₈/heavy oil system. The modified PR EOS model in conjunction with the Peneloux et al.^[148] volume translation strategy is used to predict the swelling factors for C₃H₈-heavy oil system by Li et al.^[144]. The compositions can be found in Table 1 (Feeds #8-#13). The comparison of the measured and calculated swelling factors for the aforementioned mixtures can be found elsewhere^[37,145]. As can be seen, the model is able to accurately predict the swelling factors with an AARD of 1.38% for the ten measured data points.

n-C₄H₁₀/heavy oil system. The comparison of the measured and calculated swelling factors for Feeds #5

and #6 are provided by Li and Yang^[7]. As can be seen, the swelling factors for n-C₄H₁₀/heavy oil systems are accurately predicted with an AARD of 2.78%. One exception with an AARD of 14.57% is found at 396.15 K for Feed #6, which might be caused by the experimental uncertainty. In addition, the dissolution of n-C₄H₁₀ in heavy oil can lead to a large swelling factor.

C₃H₈/n-C₄H₁₀/heavy oil system. The comparison of measured and calculated swelling factors for the aforementioned mixtures are provided by Li and Yang^[7]. The details of the experimental data can be found in Table 1 and Table 2 (Feed #7). The measured swelling factors at 298.55K, 348.35K, and 396.15K are measured to be 1.44, 1.48, and 1.50, respectively. Although saturation pressure prediction for the ternary system is not as good as that of the aforementioned binary systems, the swelling factor prediction by applying the Peneloux et al.^[148] volume translation strategy is still accurate enough with an AARD of only 1.98%.

C₃H₈/n-C₄H₁₀/CO₂/heavy oil systems. The VT technique^[148] is used to correct the molar volume obtained from the PR EOS, and then calculate the swelling factors for each of four quaternary feeds, which are tabulated in Table 1 (i.e., Feeds #23-#26)^[37,145]. The measured and predicted swelling factor of Feeds #23-#26 at temperatures from 296.45 to 373.35K are plotted in Figure 8. The predicted swelling factors agree well with the measured data, resulting in AARDs of 3.3%, 4.1%, 5.4%, and 5.2%, respectively. It is worthwhile noting that the swelling factor is found to be less sensitive to temperature compared

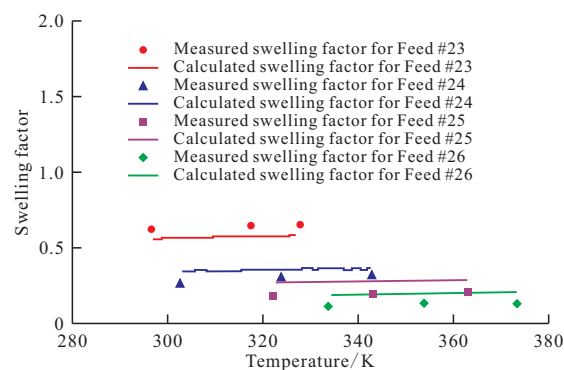


Figure 8 Comparison of the measured and predicted swelling factor for quaternary C₃H₈/n-C₄H₁₀/CO₂/heavy oil systems with Feeds #23-#26 (Modified from [37]).

with saturation pressure, while it mainly depends on the concentration of solvents dissolved in heavy oil.

DME/heavy oil system. The experimentally measured SFs for Feeds #32 and #33 with applying the VT strategy proposed by Peneloux et al.^[148] are listed in Table 2 and Figure 9. Huang et al.^[9] compared the experimentally measured and theoretically calculated SFs for the aforementioned mixtures, indicating that the experimentally measured and theoretically calculated SFs are a function of temperature for Feeds #32 and #33 with a DME concentration of 21.2 and 41.6 mol%, respectively. As can be seen, the dissolution of DME in heavy oil results in a strong swelling effect. It is found that DME has a comparable swelling effect compared with propane and CO₂, illustrating that DME can be applied as a potential alternative solvent for heavy oil recovery. In general, the thermodynamic model in combination with the VT strategy proposed by Peneloux et al.^[148] is accurate in determining the measured SFs with a reasonable RMSRE of 0.92% for two feeds of the DME/heavy-oil mixtures with a total of 10 experimental measurements.

DME/CO₂/heavy oil systems. The experimentally measured and theoretically calculated SFs for Feeds #37-#39 by employing the Péneloux VT strategy are listed in Table 2. Also, Figure 10 compares the aforementioned SFs in a temperature range of 352.25-393.95 K for Feeds #37-#39 at different DME and CO₂ concentrations. As can be clearly seen from Figure 10, the dissolution of DME and CO₂ in heavy oil leads to a strong swelling effect with SFs higher than 1.1 for all the three feeds at the tested temperatures. Also, it is found that the SFs increase slightly

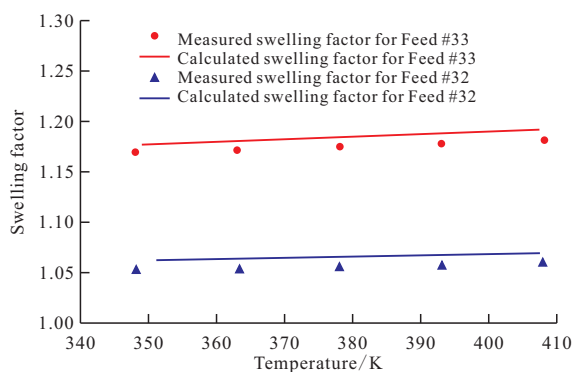


Figure 9 Comparison of the experimentally measured and theoretically predicted swelling factors for Feeds #32 and #33 (Modified from [10]).

with temperature for each feed. Compared Feed #39 with Feed #37, it is observed that the former has much higher SFs at the same temperature, though they have similar total solvent concentrations. For example, Feed #37 has an SF of 1.139 at 366.45 K, while Feed #39 has an SF of 1.162 at the same temperature. This is ascribed to the fact that DME has a stronger swelling effect than CO₂. In general, the SFs obtained by the theoretical model in this work match well with the experimental measurements.

4.3 Density

As can be seen from Table 3, it is found that both IM-E (the ideal mixing rule with effective density) and the volume-translated PR EOS are accurately enough to predict densities, while the former is better than the latter. More specifically, the volume-translated PR EOS, IM-E1 (ideal mixing rule with effective density calculated using the equation of Saryazdi^[149] or Saryazdi et al.^[150]), and IM-E2 (ideal mixing rule with effective density calculated using the equation of Chen and Yang^[40]) all yield accurate predictions of densities for the aforementioned mixtures except for the case of toluene/heavy oil/bitumen/water mixture density calculated using the volume-translated PR EOS. IM-E2 is better than IM-E1 with their AARDs of 0.73% and 1.05%, respectively, both of which are more accurate than the volume-translated PR EOS (the AARD is 1.98%). The densities of water-containing mixtures can be well predicted using the VT PR-EOS and ideal mixing rule (i.e., IM). Overall, IM-E1 underestimates most of the mixture densities, while, by tuning, IM-E2 can improve the predictions. IM-E2 works well for not only

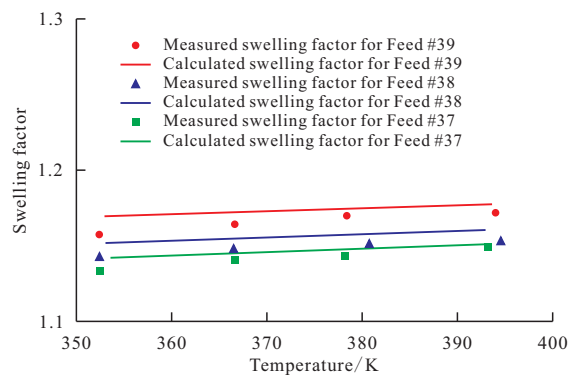


Figure 10 Comparison of the experimentally measured and theoretically predicted swelling factors for Feeds #37-#39 (Modified from [6, 10, 14]).

C₁ through *n*-C₇ and CO₂, but also N₂, toluene, and cyclohexane which have not been covered by Saryazdi^[149] and Saryazdi et al.^[150]. The tangent-line method seems to be more general (applied to more substances) and more flexible (tunable) than the extrapolation method proposed by Saryazdi^[149].

It should be noted that, for toluene-containing systems at temperatures above 450 K, the volume-translated PR EOS yields a large deviation for the predicted density, which may be due to the uniqueness of toluene/heavy oil/bitumen mixtures at high temperatures (e.g., asphaltene is soluble in toluene but insoluble in other solvents)^[40].

4.4 Viscosity

As for a gas-liquid mixture, numerous correlations have been proposed to determine the mixture viscosity, but each of them has application constraints. It is found that both the weight-based and volume-based power-law mixing rules are able to accurately predict viscosities for *n*-pentane/*n*-hexane-bitumen mixtures where the solvents are in the liquid phase^[20,151-152]. Similar conclusions can also be found through the comparison of Table 4, which shows the detailed comparisons among the weight-based, volume-based power-law mixing rules, and weight-based Cragoe's mixing rule. As can be seen from the comparison of the 258 measured viscosities listed in Table 4, the aforementioned three mixing rules together with the effective density provide good performance, while the volume-based power-law has the best accuracy with an AARD of 15.5%, followed by the weight-based power law with an AARD of 19.0%, and the weight-based Cragoe's mixing rule has the largest AARD of 32.6%^[153,154]. It is worthwhile noting that the PR EOS together with the modified alpha function and effective density makes it possible to quantify viscosity of the aforementioned mixtures as a function of pressure, temperature, and concentration with any reservoir simulators, respectively^[155,156].

4.5 Solubility

As for the database of *n*-alkane-water pairs shown in Table 5, the model developed by Chen and Yang^[38] yields good performance for the measured

X_{HC} and X_w , respectively. With respect to the predicted X_{HC} , large deviations are found for *n*-decane-water, *n*-tetradecane-water, *n*-hexadecane-water, and *n*-eicosane-water pairs, owing to the fact that few data points can be found in the literature to develop the prediction models. With regard to the predicted X_w , accurate predictions can be found except for propane-water, *n*-butane-water, and *n*-hexadecane-water pairs. This is because propane and *n*-butane are more volatile than heavier hydrocarbons.

4.6 Mass Transfer

Mass transfer without coupling heat transfer. A novel methodology developed by Li and Yang^[114] is used to calculate the molecular-diffusion coefficient for each component of the solvent/CO₂ mixture in heavy oil under reservoir conditions based on the pressure-decay method. A total of three diffusion test data for pure-CO₂/heavy-oil system, C₃H₈/CO₂/heavy-oil system, and *n*-C₄H₁₀/CO₂/heavy-oil system (i.e., Feeds #42-#44 in Table 6) are collected from the literature^[114]. Theoretically, the volume-translated PR EOS with a modified alpha function combined with a 1D diffusion model is used to improve its accuracy. As seen from Table 7^[144], there is an excellent agreement between the calculated and measured mole fractions of the aforementioned systems at the end of diffusion tests, indicating that the applicability of the newly proposed method.

As can also be seen, the mole fractions obtained by using individual molecular diffusion coefficients and apparent diffusion coefficient for gas mixtures are both listed by Li and Yang^[114]. It is found that the former can be used to reproduce the measured pressure profiles with a better accuracy than the latter. Physically, each component in a gas mixture shall diffuse differently in heavy oil due to its different physical properties. This is why one must treat separately the molecular diffusion coefficient of each component in a gas mixture to reproduce the measured compositions together with other measured parameters as a function of time during a diffusion test. In addition, the methodology is further validated by another study performed by Zheng et al.^[131,157] by comparing the measured and calculated swelling factors for solvent/

CO₂/heavy oil systems with apparent/individual diffusion coefficients.

Jang and Yang^[158] determined the effective diffusivity of individual gas components of a binary gas mixture in a porous medium saturated with heavy oil without consideration of the concentration-dependent contribution, while the effective diffusivity is significantly affected by the pore size and shape, tortuosity, and the gas compositions and properties.

In summary, Li and Yang^[114] proposed a robust methodology by combining the PR EOS with a 1D diffusion model on the basis of the pressure-decay theory which can be used to accurately determine the molecular diffusion coefficient for each component of the solvent/CO₂ mixture in heavy oil under reservoir conditions. Subsequently, Jang et al.^[124] proposed a robust methodology with its wide applicability and high accuracy to determine the diffusivity of CO₂ by treating it as an exponential function of gas concentration with consideration of oil swelling.

Mass transfer with coupling heat transfer. Based on the newly proposed alpha function^[49], Zheng^[159] developed a generalized methodology to accurately quantify diffusion coefficients of a CO₂/heavy oil system, an *n*-C₄H₁₀/heavy oil system, an *n*-C₄H₁₀/CO₂/heavy oil system, and a C₃H₈/*n*-C₄H₁₀/CO₂/heavy oil system by coupling heat and mass transfer and treating heavy oil as multiple PCs. The details of the experimental database can be found in Tables 6 and 7 (Feeds #45-#47).

The measured and calculated dynamic swelling factors based respectively on (a) constant diffusion coefficient and (b) diffusion coefficient as a function of viscosity and as a constant for Feeds #45-#47 are reported by Zheng et al.^[131]. As can be seen, the calculated results are in a good agreement with the measured ones, while the latter is more accurate than the former, indicating that it is better to assume CO₂ diffusion coefficient as a function of viscosity during the coupled heat and mass transfer stage.

Based on the methodology developed by Sun et al.^[116], further modifications have been made by introducing C₃H₈ into hot CO₂-heavy oil systems^[131]. More specifically, a 2D heat and mass transfer model

incorporated into the volume-translated PR EOS with a modified alpha function has been developed to describe the coupling heat and mass transfer for the aforementioned systems. Heavy oil is treated as multiple PCs instead of a single PC^[116]. The details of the experimental database can be found in Tables 6 and 7 (Feeds #48-#50).

The measured dynamic swelling factors and the calculated ones based on the determined individual diffusion coefficients and apparent diffusion coefficients for Feeds #48-#50 are made available elsewhere^[133]. As can be seen, the calculated dynamic swelling factors are in a good agreement with the measured ones, implying that the aforementioned method is applicable for such alkane/CO₂/heavy oil systems.

Experimental and theoretical techniques have been made by Zheng et al.^[157] to determine individual diffusion coefficients of alkane solvents and CO₂ in heavy oil at high pressures and elevated temperatures for the Feeds #46 and #51-#53 as listed in Table 6. Zheng and Yang^[117] proposed the DVA to determine the individual diffusion coefficients for C₃H₈/*n*-C₄H₁₀/CO₂/heavy oil systems by coupling heat and mass transfer as well as by treating heavy oil as multiple PCs.

The dynamic swelling factors based on the individual and apparent diffusion coefficients for Feeds #46 and #51-#53 are provided by Zheng and Yang^[117] and Zheng^[159]. As can be seen, there exists a good agreement between the calculated and measured dynamic swelling factors. In addition, the measured and calculated mole fractions of Feeds #52 and #53 at the end of diffusion tests based on the individual diffusion coefficients further verify the accuracy of the method from a different angle^[159]. For a given solvent/heavy oil system, heat transfer is found to achieve equilibrium state much fast than mass transfer.

In summary, Sun et al.^[116] proposed a generalized methodology to couple heat and mass transfer of both a pure gas-heavy oil system and a mixture gas-heavy oil system at high pressures and elevated temperatures. More specifically, the PR EOS together with a one-way heat and mass transfer model has

been developed to couple heat and mass transfer of CO_2 /heavy oil system and $\text{CO}_2/\text{C}_3\text{H}_8$ /heavy oil system under a constant pressure condition. Some findings are worth mentioning: 1). Heat transfer is discovered to be faster than mass transfer, resulting in thermal equilibrium being reached faster than mass equilibrium; 2). The heavy oil expands fast during the first step of the coupled heat and mass transfer, then progressively swells during the subsequent mass transfer stage; and 3). The addition of C_3H_8 to the CO_2 stream improves mass diffusion as well as heat diffusion, resulting in an enhanced swelling effect of heavy oil. Subsequently, the aforementioned methodology is further validated by characterizing heavy oil as multiple PCs as well as introducing a 2D heat and mass transfer model to replace the 1D model to improve its accuracy^[115,117,131,160]. Recently, we have developed techniques to quantify the preferential mass transfer of each component of a binary or ternary gas mixture into heavy oil at high pressures and elevated temperatures by considering both concentration dependence and the presence of porous media^[160-161].

4.7 Nonequilibrium Phase Behaviour

Nonequilibrium CCE experiments at a constant volume expansion rate. Based on the proposed α function^[49], a robust and pragmatic technique has been developed to experimentally and theoretically quantify the nonequilibrium phase behaviour of alkane solvent (s)/ CO_2 /heavy oil systems under reservoir conditions^[132-136]. More specifically, a total of ten constant CCE experiments with a constant volume expansion rate are made for quantifying the nonequilibrium phase behaviour of CO_2 /heavy oil systems, CH_4 /heavy oil systems, and $\text{CO}_2/\text{C}_3\text{H}_8$ /heavy oil systems, while the details of these experiments are tabulated in Table 8 (Feeds #54-#56). The measured and calculated pressure curves for each of the aforementioned three mixtures are made available by Shi et al.^[132,162] and Shi^[163]. It is found that the calculated pressure profiles match the measured ones quite well, indicating the accuracy of the mathematical model proposed by Shi et al.^[132,134,162,164], Zhao et al.^[165], and Dong et al.^[166] Subsequently, it is further applied to determine the properties of foamy oil (i.e., compress-

ibility and density), which can be found elsewhere^[132,133,162].

Nonequilibrium CCE experiments with a constant pressure decline rate. With a total of six CCE experiments with a constant pressure decline rate, theoretical models based on the PR EOS have been developed to quantify the nonequilibrium phase behaviour of CO_2 /heavy oil systems, CH_4/CO_2 /heavy oil systems, and $\text{CH}_4/\text{C}_3\text{H}_8$ /heavy oil systems^[133-135], while their corresponding database are tabulated in Table 9 (Feeds #57-#59). Good agreements can be found between the calculated and measured volume-pressure profiles under nonequilibrium conditions, implying the accuracy of the proposed mathematical models^[132-134].

Two important ways to achieving nonequilibrium conditions for the aforementioned systems are constant pressure decrease rate and constant volume expansion rate, each of which has its distinct advantages and limitations^[133]. Also, it is worthwhile noting that the PR EOR together with the modified alpha function makes it possible to determine the nonequilibrium phase behaviour and physical properties of the aforementioned mixtures by integrating with any reservoir simulators.

A single-gas bubble growth. A mechanistic model has been developed by Shi et al.^[135] for quantifying a single gas bubble growth with considering multicomponent gas diffusion in solvent(s)/ CO_2 /heavy oil systems under nonequilibrium conditions. Experimentally, CCE experiments are conducted for $\text{C}_3\text{H}_8/\text{CO}_2$ /heavy oil systems under equilibrium and nonequilibrium conditions, respectively. Theoretically, the modified PR EOS^[49] together with other relative equations (i.e., the classic continuity equation, motion equation, diffusion - convection equation, and real gas equation) are used to improve the accuracy of the model. The comparison between the measured gas bubble radii and those calculated with the previously mentioned model shows an excellent agreement (see Figure 11), which demonstrates the accuracy of using the model to determine the underlying mechanisms of gas bubble growth in the aforementioned systems. Also, such experimental measurements col-

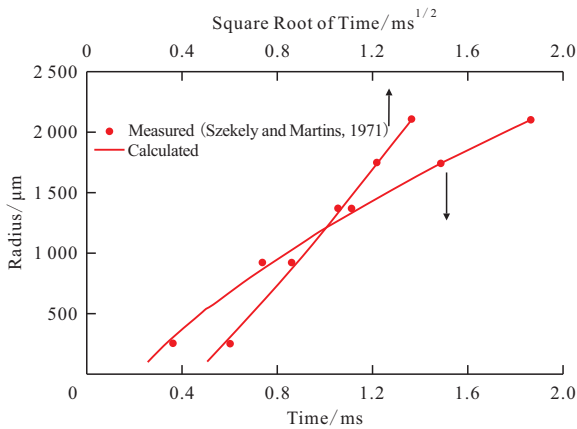


Figure 11 Comparison of the measured and calculated bubble radius for $n\text{-C}_5\text{H}_{12}/n\text{-C}_{14}\text{H}_{30}$ systems (Modified from [135, 164]).

lected from the literature are not sufficient to determine the critical nucleus radius which is defined as the initial value of gas bubble radius during the period of a stable bubble growth, though the new model has been validated with the measured bubble radius.

Dynamic volume. Based on the mechanistic model of a single-gas bubble growth developed by Shi and Yang^[135], a novel and robust technique has been developed to determine the dynamic volume growth of multi-component gas bubbles with consideration of preferential mass transfer of each gas component in alkane solvent (s)/CO₂/heavy oil systems under nonequilibrium conditions. Combined with the newly proposed mechanistic model, a volume equation is incorporated into an equation matrix to theoretically describe the kinetics of multicomponent gas bubbles growth. Such an equation matrix is then solved to match the pressure-volume as a function of time measured with CCE tests under nonequilibrium conditions, allowing for determining the dynamic volume of gas bubbles by taking the preferential diffusion of each component in a gas mixture into account. Subsequently, dynamic composition and volume of evolved gas in foamy oil can be quantified and analyzed. On the basis of the matched experimental measurements, sensitivity analysis has been performed to numerically examine supersaturation pressure, pressure decline rate, and amount of each gas component on the growth of gas bubbles.

As depicted in Figure 12, there exist excellent agreements between the measured volume-pressure profiles and calculated ones with the newly proposed

models. The compositions of CH₄ and CO₂ in evolved gas at the end of experimental duration are calculated to be 45.9 mol% and 54.1 mol%, respectively, which is very close to their corresponding experimental measurements of 47.2 mol% and 51.6 mol% with a respective deviation of 2.8% and 4.8%. Both of the aforementioned results confirm that the newly developed model can be used to effectively and accurately capture the essentially time-dependent volume of foamy oil.

Accordingly, the dynamic mole compositions of evolved gas in CH₄/CO₂/heavy oil systems and CH₄/C₃H₈/heavy oil systems can be obtained on the basis of the computed concentration distribution in the liquid phase (see Figure 13). It is worthwhile noting that, as for CH₄/CO₂/heavy oil systems, the calculated compositions of two gases are very close to the measured ones at the end of the experiment, which further confirms the reliability of the newly developed technique for determining dynamic compositions of

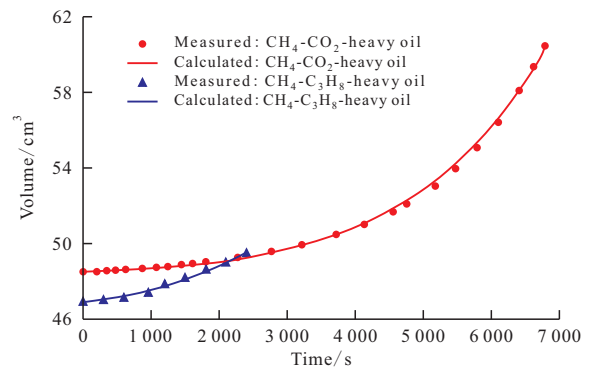


Figure 12 Measured and calculated liquid volumes of CH₄/CO₂/heavy oil systems (Feed #59) and CH₄/C₃H₈/heavy oil systems (Feed #58) below the pseudo-bubblepoint pressure under nonequilibrium conditions (Modified from [135, 163])

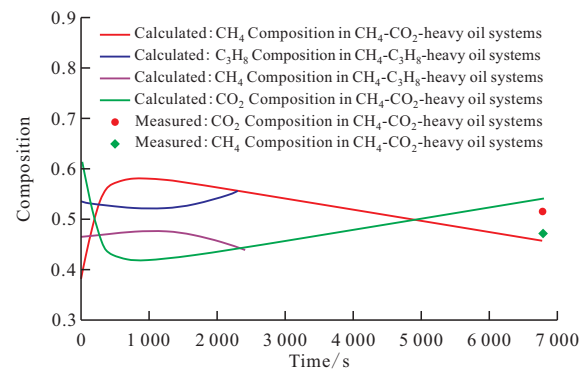


Figure 13 Measured and calculated dynamic composition of each gas component in evolved gas for CH₄/CO₂/heavy oil systems (Feed #59) and CH₄/C₃H₈/heavy oil systems (Feed #58), respectively (Modified from [163])

the aforementioned systems.

5 Conclusions

In this work, significant improvements on accurately quantifying phase behaviour and physical properties of solvents/ CO_2 /water/heavy oil systems under equilibrium and nonequilibrium conditions are critically reviewed. Specific findings are listed as follows: First, new alpha functions for hydrocarbon and water in the PR EOS have been respectively developed to more accurately predict the vapor pressure of pure hydrocarbon compounds and water, respectively. The acentric factor is redefined at a reduced temperature of 0.6 and incorporated into the newly developed alpha function, which can further improve the prediction accuracy. By treating heavy oil as a single PC, three BIP correlations in the PR EOS are proposed for characterizing CO_2 /heavy oil binaries, C_3H_8 /heavy oil binaries, and $n\text{-C}_4\text{H}_{10}$ /heavy oil binaries, respectively. The PR EOS together with the BIP correlations and the new alpha function is able to describe the phase behaviour and physical properties of solvent(s)/ CO_2 /water/heavy oil systems with a generally good accuracy, including multiphase boundaries (or pseudo-bubble-point pressures), density, viscosity, (mutual) solubility, and preferential mass transfer. As for mass transfer, the volume-translated PR EOS with the modified alpha function combined with a 1D diffusion model is able to improve the accuracy for calculating the molecular-diffusion coefficient for each component of the solvent/ CO_2 mixture in heavy oil under reservoir conditions based on the pressure-decay method. Heat and mass transfer are investigated under a constant pressure system, while the 1D diffusion model is further improved as 2D for a much better prediction accuracy.

Acknowledgements: The authors acknowledge a Discovery Development Grant, a Discovery Grant, and a Collaborative and Research Development (CRD) Grant awarded to D. Yang from the Natural Sciences and Engineering Research Council (NSERC) of Canada, a Mitacs Industry-Faculty Collaboration for Innovation (MIFCI) Award, and financial sup-

port from EHR Enhanced Hydrocarbon Recovery Inc. and Thermal Recovery Technologies Inc.

Nomenclature

a	— attraction parameter defined in PR EOS
A	— aqueous phase
b	— van der Waals volume, m^3/kmol
λ	— EOS- dependent parameter
g_{ij}	— energy parameter, J/mol
G_{∞}^E	— excess Gibbs free energy at infinite pressure, J/mol
L	— oleic phase
P	— pressure, kPa
P_b	— bubblepoint pressure, kPa
P_{sb}	— pseudo-bubblepoint pressure, kPa
P_s	— apparent critical supersaturation pressure, kPa
SF	— swelling factor
SG	— specific gravity
T	— temperature, K
T_r	— reduced temperature
V	— vapour phase
y_i	— mole fraction of the i th component
$\alpha(T_r, \omega)$	— alpha function in the PR EOS
α_{ij}	— non-randomness parameter
δ	— BIP (binary interaction parameter)
$\gamma_{i\infty}$	— activity coefficient
ρ_o	— density of heavy oil, kg/m^3
ω	— acentric factor

References

- [1] Tg Othman T. R., El Emam, M. M., Tewari R. D., Ramli A. S., Anasir N., Rahman M. Izzat A, Sulleh, S., and Ahmed, S. M. 2013. Cold Heavy Oil Development: Learn from the Past, Plan for the Future. Paper SPE-165449-MS, presented at the SPE Canada Heavy Oil Conference, Calgary, AB, 11-13 June. <https://doi.org/10.2118/165449-MS>.
- [2] Meyer R. F., Attanasi E. D., and Freeman P. A. 2007. Heavy Oil and Natural Bitumen Resources in Geological Basins of the World. Open-File Report 2007-1084, U.S. Geological Survey, Denver, CO. <http://pubs.usgs.gov/of/2007/1084/>.
- [3] Alberta Energy Regulator. 2021. *Alberta Energy Resource Industries Monthly Statistics: Oil Supply & Disposition*. Statistical Reports, Calgary, AB.
- [4] Jha R. K., Kumar M., Benson I., and Hanzlik E. 2013. New Insights into Steam/Solvent-Coinjection-Process Mechanism. *SPE Journal* 18 (5): 867-877. <https://doi.org/10.2118/159277-PA>.
- [5] Liu H. and Cheng L., Huang S., Jia P., and Xiong H. 2018. Heat and Mass Transfer Characteristics of Superheated Fluid for Hybrid Solvent-Steam Process in Perforated Horizontal Wellbores. *International Journal of Heat and Mass Transfer* 122: 557-

573. <https://doi.org/10.1016/j.ijheatmasstransfer.2018.02.005>.
- [6] Liu H., Cheng L., Wu K., Huang S., and Maini B. 2018. Assessment of Energy Efficiency and Solvent Retention Inside Steam Chamber of Steam- and Solvent-Assisted Gravity Drainage Process. *Applied Energy* 226: 287-299. <https://doi.org/10.1016/j.apenergy.2018.06.017>.
- [7] Li, H. and Yang, D. 2013. Phase Behaviour of $C_3H_8/n-C_4H_{10}$ /Heavy-Oil Systems at High Pressures and Elevated Temperatures. *Journal of Canadian Petroleum Technology* 52 (1) : 30-40. <https://doi.org/10.2118/157744-PA>.
- [8] Sheng K., Okuno R., and Wang M. 2018. Dimethyl Ether as an Additive to Steam for Improved Steam-Assisted Gravity Drainage. *SPE Journal* 23 (4) : 1201-1222. <https://doi.org/10.2118/184983-PA>.
- [9] Huang D., Li R., and Yang D. 2021. Multiphase Boundaries and Physical Properties of Solvents/Heavy Oil Systems under Reservoir Conditions by Use of Isenthalpic Flash Algorithms. *Fuel* 298: 120508. <https://doi.org/10.1016/j.fuel.2021.120508>.
- [10] Huang D., Li R., and Yang D. 2021. Phase Behaviour and Physical Properties of Dimethyl Ether (DME)/Water/Heavy Oil Systems under Reservoir Conditions. *SPE Journal* 26 (4) : 2380-2396. SPE-205353-PA. <https://doi.org/10.2118/205353-PA>.
- [11] Zargar Z. and Farouq Ali S. F. 2021. Solvent Co-injection with Steam-Assisted Gravity Drainage Process Performance Evaluation-New Analytical Treatment in Relation to Constant Injection Rate. *International Journal of Heat and Mass Transfer* 65: 120679. <https://doi.org/10.1016/j.ijheatmasstransfer.2020.120679>.
- [12] Zhao M., Yang S., and Yang D. 2022. Performance Evaluation of Hybrid Steam-Solvent Processes in a Post-CHOPS Reservoir with Consideration of Wormhole Network. *Journal of Energy Resources Technology* 144 (4) : 043001. <https://doi.org/10.1115/1.4051552>.
- [13] Maini B., Sarma H. K., and George A. E. 1993. Significance of Foamy-Oil Behaviour in Primary Production of Heavy Oils. *Journal of Canadian Petroleum Technology* 32 (9) : 50-54. <https://doi.org/10.2118/93-09-07>.
- [14] Maini B. 1996. Foamy Oil Flow in Heavy Oil Production. *Journal of Canadian Petroleum Technology* 35 (6) : 21-24. <https://doi.org/10.2118/96-06-01>.
- [15] Maini B. 2001. Foamy-Oil Flow. *Journal of Canadian Petroleum Technology* 53 (10) : 54-64. <https://doi.org/10.2118/68885-JPT>.
- [16] Mehrotra A. K. and Svrcek W. Y. 1998. Properties of Cold Lake Bitumen Saturated with Pure Gases and Gas Mixtures. *The Canadian Journal of Chemical Engineering* 66 (4) : 656-665. <https://doi.org/10.1002/cjce.5450660419>.
- [17] Nourozieh H., Kariznovi M., and Abedi J. 2016. Measurement and Evaluation of Bitumen/Toluene-Mixture Properties at Temperatures up to 190°C and Pressures up to 10 MPa. *SPE Journal* 21 (5) : 1705-1720. <https://doi.org/10.2118/180922-PA>.
- [18] Nourozieh H., Kariznovi M., and Abedi J. 2016. Measurement and Modeling of Solubility and Saturated-Liquid Density and Viscosity for Methane/Athabasca-Bitumen Mixtures. *SPE Journal* 21 (1) : 180-189. <https://doi.org/10.2118/174558-PA>.
- [19] Amani M. J., Gray M. R., and Shaw J. M. 2014. The Phase Behavior of Athabasca Bitumen + Toluene + Water Ternary Mixtures. *Fluid Phase Equilibria* 370: 75-84. <https://doi.org/10.1016/j.fluid.2014.02.028>.
- [20] Gao J., Okuno R., and Li H. 2018. A Phase-Behavior for *n*-hexane/Bitumen and *n*-octane/Bitumen Mixtures. *SPE Journal* 23 (1) : 128-144. <https://doi.org/10.2118/186097-PA>.
- [21] Li H., Zheng S., and Yang D. 2013. Enhanced Swelling Effect and Viscosity Reduction of Solvent(s)/CO₂/Heavy-Oil Systems. *SPE Journal* 18 (4) : 695-707. <https://doi.org/10.2118/150168-PA>.
- [22] Li, X. and Yang, D. 2013. Determination of Mutual Solubility between CO₂ and Water by Using the Peng-Robinson Equation of State with Modified Alpha Function and Binary Interaction Parameter. *Industrial & Engineering Chemistry Research* 52 (38) : 13829-13838. <https://doi.org/10.1021/ie401365n>.
- [23] Nourozieh H., Kariznovi M., and Abedi J. 2015. Density and Viscosity of Athabasca Bitumen Samples at temperatures up to 200°C and Pressures up to 10 MPa. *SPE Reservoir Evaluation & Engineering* 18 (3) : 375-386. <https://doi.org/10.2118/176026-PA>.
- [24] Nourozieh H., Kariznovi M., and Abedi J. 2015. Experimental and Modeling Studies of Phase Behavior for Propane/Athabasca Bitumen Mixtures. *Fluid Phase Equilibria* 397: 37-43. <https://doi.org/10.1016/j.fluid.2015.03.047>.
- [25] Nourozieh H., Kariznovi M., and Abedi J. 2015. Modeling and Measurement of Thermo-Physical Properties for Athabasca Bitumen and *n*-Heptane Mixtures. *Fuel* 157: 73-81. <https://doi.org/10.1016/j.fuel.2015.04.032>.
- [26] Nourozieh H., Kariznovi M., and Abedi J. 2017. Solubility of *n*-butane in Athabasca Bitumen and Saturated Densities and Viscosities at Temperatures up to 200°C. *SPE Journal* 22 (1) : 94-102. <https://doi.org/10.2118/180927-PA>.
- [27] Gao J., Okuno R., and Li H. 2017. An Experimental Study of Multiphase Behavior for *n*-butane/Bitumen/Water Mixtures. *SPE Journal* 22 (3) : 783-798. <https://doi.org/10.2118/180736-PA>.
- [28] Baek K. H., Sheng K., Argüelles-Vivas F. J., and Okuno R. 2019. Comparative Study of Oil-Dilution Capability of Dimethyl Ether and Hexane as Steam Additives for Steam-Assisted Gravity Drainage. *SPE Reservoir Evaluation & Engineering* 22 (3) : 1030-1048. <https://doi.org/10.2118/187182-PA>.
- [29] Ratnakar R. R., Dindoruk B., and Wilson L. 2016. Experimental Investigation of DME-Water-Crude Oil Phase Behavior and PVT Modeling for the Application of DME-Enhanced Waterflooding. *Fuel* 182 (15) : 188-197. <https://doi.org/10.1016/j.fuel.2016.05.096>.
- [30] Ratnakar R. R., Dindoruk B., and Wilson L. C. 2017. Development of Empirical Correlation for DME-Partitioning Between Brine and Crudes for Enhanced Waterflooding Applications. *Journal of Petroleum Science and Engineering* 157: 264-272. <https://doi.org/10.1016/j.petrol.2017.07.029>.
- [31] Ratnakar R. R., Dindoruk B., and Wilson L. C. 2017. Phase Behavior Experiments and PVT Modeling of DME-Brine-Crude Oil Mixtures Based on Huron-Vidal Mixing Rules for EOR Applications. *Fluid Phase Equilibria* 434 (25) : 49-62. <https://doi.org/10.1016/j.fluid.2016.11.021>.

- [32] Shu, W. R. and Hartman, K. J. 1988. Effect of Solvent on Steam Recovery of Heavy Oil. *SPE Reservoir Engineering* 3 (2): 457-465. <https://doi.org/10.2118/14223-PA>.
- [33] Glandt C. A. and Chapman W. G. 1995. The Effect of Water Dissolution on Oil Viscosity. *SPE Reservoir Evaluation & Engineering* 10 (1): 59-64. <https://doi.org/10.2118/24631-PA>.
- [34] Luo, S. and Barrufet, M. A. 2005. Reservoir Simulation Study of Water-in-Oil Solubility Effect on Oil Recovery in Steam Injection Process. *SPE Reservoir Evaluation & Engineering* 8 (6): 528-533. <https://doi.org/10.2118/89407-PA>.
- [35] Amani M. J., Gray M. R., and Shaw J. M. 2013. Phase Behavior of Athabasca Bitumen + Water Mixtures at High Temperature and Pressure. *The Journal of Supercritical Fluids* 77: 142-152. <https://doi.org/10.1016/j.supflu.2013.03.007>.
- [36] Li X., Han H., Yang D., Liu X., and Qin J. 2017. Phase Behavior of C_3H_8 - CO_2 -Heavy Oil Systems in the Presence of Aqueous Phase under Reservoir Conditions. *Fuel* 209: 358-370. <https://doi.org/10.1016/j.fuel.2017.08.010>.
- [37] Li X., Yang D., and Fan Z. 2017. Vapor-Liquid Phase Boundaries and Swelling Factors of C_3H_8 - n - C_4H_{10} - CO_2 -Heavy Oil Systems under Reservoir Conditions. *Fluid Phase Equilibria* 434: 211-221. <https://doi.org/10.1016/j.fluid.2016.12.004>.
- [38] Chen Z. and Yang D. 2018. Quantification of Phase Behaviour of Solvents-Heavy Oil Systems in the Presence of Water at High Pressures and Elevated Temperatures. *Fuel* 232: 803-816. <https://doi.org/10.1016/j.fuel.2018.05.116>.
- [39] Li H., Yang D., and Li X. 2012. Determination of Three-Phase Boundaries of Solvent(s)- CO_2 -Heavy Oil Systems under Reservoir Conditions. *Energy & Fuels* 27 (1): 145-153. <https://doi.org/10.1021/ef301549a>.
- [40] Chen Z. and Yang D. 2020. A Tangent-Line Approach for Effective Density Used in Ideal Mixing Rule: Part I-Prediction of Density for Heavy Oil/Bitumen Associated Systems. *SPE Journal* 25 (3): 1140-1154. <https://doi.org/10.2118/199340-PA>.
- [41] Chen Z., Zhao Z., and Yang D. 2020. Quantification of Phase Behaviour for Solvent/Heavy-Oil/Water Systems at High Pressures and Elevated Temperatures with Dynamic Volume Analysis. *SPE Journal* 25 (6): 2915-2931. <https://doi.org/10.2118/201240-PA>.
- [42] Pina-Martinez A., Privat R., Jaubert J., and Peng D. 2019. Updated Versions of the Generalized Soave α -Function Suitable for the Redlich-Kwong and Peng-Robinson Equations of State. *Fluid Phase Equilibria* 485: 264-269. <https://doi.org/10.1016/j.fluid.2018.12.007>.
- [43] Peng D. Y. and Robinson D. B. 1976. A New Two-Constant Equation of State. *Industrial & Engineering Chemistry Fundamentals* 15 (1): 59-64. <https://doi.org/10.1021/i160057a011>.
- [44] Soave G. 1972. Equilibrium Constants from a Modified Redlich-Kwong Equation of State. *Chemical Engineering Science* 27 (6): 1197-1203. [https://doi.org/10.1016/0009-2509\(72\)80096-4](https://doi.org/10.1016/0009-2509(72)80096-4).
- [45] Trebble M. A. and Bishnoi P. R. 1987. Development of a New Four-Parameter Cubic Equation of State. *Fluid Phase Equilibria* 35 (1): 1-18. [https://doi.org/10.1016/0378-3812\(87\)80001-8](https://doi.org/10.1016/0378-3812(87)80001-8).
- [46] Twu C. H., Bluck D., Cunningham J. R., and Coon J. E. 1991. A Cubic Equation of State with a New Alpha Function and a New Mixing Rule. *Fluid Phase Equilibria* 69 (10): 33-50. [https://doi.org/10.1016/0378-3812\(91\)90024-2](https://doi.org/10.1016/0378-3812(91)90024-2).
- [47] Twu C. H., Coon J. E., and Cunningham J. R. 1995. A New Generalized Alpha Function for a Cubic Equation of State: Part 1. Peng-Robinson Equation. *Fluid Phase Equilibria* 105 (1): 49-59. [https://doi.org/10.1016/0378-3812\(94\)02601-V](https://doi.org/10.1016/0378-3812(94)02601-V).
- [48] Twu C. H., Coon J. E., and Cunningham J. R. 1995. A New Generalized Alpha Function for a Cubic Equation of State: Part 2. Redlich-Kwong Equation. *Fluid Phase Equilibria* 105 (1): 61-69. [https://doi.org/10.1016/0378-3812\(94\)02602-W](https://doi.org/10.1016/0378-3812(94)02602-W).
- [49] Li, H. and Yang, D. 2011. Modified α Function for Peng-Robinson Equation of State to Improve Vapour Pressure Prediction of Non-hydrocarbon and Hydrocarbon Compounds. *Energy & Fuels* 25 (1): 215-223. <https://doi.org/10.1021/ef100927z>.
- [50] Mathias P. M. 1983. A Versatile Phase Equilibrium Equation of State. *Industrial and Engineering Chemistry Product Research and Development* 22 (3): 385-391. <https://doi.org/10.1021/i200022a008>.
- [51] Mathias P. M. and Copeman T. W. 1983. Extension of the Peng-Robinson Equation of State to Complex Mixtures: Evaluation of the Various Forms of the Local Composition Concept. *Fluid Phase Equilibria* 13: 91-108. [https://doi.org/10.1016/0378-3812\(83\)80084-3](https://doi.org/10.1016/0378-3812(83)80084-3).
- [52] Stryjek R. and Vera J. H. 1986. PRSV: An Improved Peng-Robinson Equation of State for Pure Compounds and Mixtures. *The Canadian Journal of Chemical Engineering* 64 (2): 323-333. <https://doi.org/10.1002/cjce.5450640224>.
- [53] Melhem G. A., Saini R., and Goodwin B. M. 1989. A Modified Peng-Robinson Equation of State. *Fluid Phase Equilibria* 47 (2-3): 189-237. [https://doi.org/10.1016/0378-3812\(89\)80176-1](https://doi.org/10.1016/0378-3812(89)80176-1).
- [54] Hernández-Garduza O., García-Sánchez F., Ápam-Martínez D., and Vázquez-Román R. 2002. Vapor Pressures of Pure Compounds Using the Peng-Robinson Equation of State with Three Different Attractive Terms. *Fluid Phase Equilibria* 198 (2): 195-228. [https://doi.org/10.1016/S0378-3812\(01\)00765-8](https://doi.org/10.1016/S0378-3812(01)00765-8).
- [55] Neau E., Hernández-Garduza O., Escandell J., Nicolas C., and Raspo I. 2009. The Soave, Twu and Boston-Mathias Alpha Functions in Cubic Equations of State: Part I. Theoretical Analysis of their Variations According to Temperature. *Fluid Phase Equilibria* 276 (2): 87-93. <https://doi.org/10.1016/j.fluid.2008.09.023>.
- [56] Neau E., Raspo I., Escandell J., Nicolas C., and Hernández-Garduza O. 2009. The Soave, Twu and Boston-Mathias Alpha Functions in Cubic Equations of State: Part II. Modeling of Thermodynamic Properties of Pure Compounds. *Fluid Phase Equilibria* 276 (2): 156-164. <https://doi.org/10.1016/j.fluid.2008.10.010>.
- [57] Heyen G. 1981. A Cubic Equation of State with Extended Range of Application. *Proceedings of the 2nd World Congress of Chemical Engineering*, Montreal, QC, 4-9 October.
- [58] Peng D. Y. and Robinson D. B. 1976. Two and Three Phase Equilibrium Calculations for Systems Containing Water. *The Canadian Journal of Chemical Engineering* 54 (5): 595-599. <https://doi.org/10.1002/cjce.5450540509>.

- doi.org/10.1002/cjce.5450540541
- [59] Peng D. Y. and Robinson D. B. 1980. Two- and Three-Phase Equilibrium Calculations for Coal Gasification and Related Processes. Thermodynamics of Aqueous Systems with Industrial Applications. ACS Symposium Series, American Chemical Society, Washington, DC. <https://doi.org/10.1021/bk-1980-0133.ch020>.
- [60] Søreide, I. Whitson, C. H. 1992. Peng-Robinson Prediction for Hydrocarbons, CO₂, N₂, and H₂S with Pure Water and NaCl Brine. *Fluid Phase Equilibria* 77 (15) : 217-240. [https://doi.org/10.1016/0378-3812\(92\)85105-H](https://doi.org/10.1016/0378-3812(92)85105-H).
- [61] Zhao W., Xia L., Sun X., and Xiang S. 2019. A Review of the Alpha Functions of Cubic Equations of State for Different Research Systems. *International Journal of Thermophysics* 40 (12). <https://doi.org/10.1007/s10765-019-2567-4>.
- [62] Pitzer K. S. 1955. The Volumetric and Thermodynamic Properties of Fluids: I. Theoretical Basis and Virial Coefficients. *Journal of the American Chemical Society* 77 (13) : 3427-3433. <https://doi.org/10.1021/ja01618a001>.
- [63] Graboski M. S. and Daubert T. E. 1978. A Modified Soave Equation of State for Phase Equilibrium Calculations. 2. Systems Containing CO₂, H₂S, N₂, and CO. *Industrial and Engineering Chemistry Process Design and Development* 17 (4) : 448-454. <https://doi.org/10.1021/i260068a010>.
- [64] Soave G. 1993. Improving the Treatment of Heavy Hydrocarbons by the SRK EOS. *Fluid Phase Equilibria* 84: 339-342. [https://doi.org/10.1016/0378-3812\(93\)85131-5](https://doi.org/10.1016/0378-3812(93)85131-5).
- [65] Lee, B. Kesler, M. 1975. A Generalized Thermodynamic Correlation based on Three-Parameter Corresponding States. *American Institute of Chemical Engineers* 21 (3) : 510-527. <https://doi.org/10.1002/aic.690210313>.
- [66] Pitzer K. S., Lippmann D. Z., Curl R. F., Huggins C. M., and Petersen D. E. 1955. The Volumetric and Thermodynamic Properties of Fluids: II. Compressibility Factor, Vapor Pressure and Entropy of Vaporization. *Journal of the American Chemical Society* 77 (13) : 3433-3440. <https://doi.org/10.1021/ja01618a002>.
- [67] Twu C.H., Coon J. E., and Cunningham J. R. 1994. A Generalized Vapor Pressure Equation for Heavy Hydrocarbons. *Fluid Phase Equilibria* 96 (10) : 19-31. [https://doi.org/10.1016/0378-3812\(94\)80085-5](https://doi.org/10.1016/0378-3812(94)80085-5).
- [68] Nji G. N., Svrcek W. Y., Yarranton H., and Satyro M. A. 2009. Characterization of Heavy Oils and Bitumens 2. Improving the Prediction of Vapor Pressures for Heavy Hydrocarbons at Low Reduced Temperatures Using the Peng-Robinson Equation of State. *Energy & Fuels* 23 (1) : 366-373. <https://doi.org/10.1021/ef8006855>.
- [69] Chen Z. and Yang D. 2017. Optimization of the Reduced Temperature Associated with Peng-Robinson Equation of State and Soave-Redlich-Kwong Equation of State to Improve Vapor Pressure Prediction for Heavy Hydrocarbon Compounds. *Journal of Chemical and Engineering Data* 62 (10) : 3488-3500. <https://doi.org/10.1021/acs.jced.7b00496>.
- [70] Gao W., Robinson R. L., and Gasem K. A. M. 2003. Alternate Equation of State Combining Rules and Interaction Parameter Generalizations for Asymmetric Mixtures. *Fluid Phase Equilibria* 213 (1-2) : 19-37. [https://doi.org/10.1016/S0378-3812\(03\)00123-7](https://doi.org/10.1016/S0378-3812(03)00123-7).
- [71] Valderrama J. O. and Zavaleta J. 2005. Generalized Binary Interaction Parameters in the Wong-Sandler Mixing Rules for Mixtures Containing n-alkanols and Carbon Dioxide. *Fluid Phase Equilibria* 234 (1-2) : 136-143. <https://doi.org/10.1016/j.fluid.2005.05.020>.
- [72] Fateen S. E. K., Khalil M. M., and Elnabawy A. O. 2013. Semi-Empirical Correlation for Binary Interaction Parameters of the Peng-Robinson Equation of State with the van der Waals Mixing Rules for the Prediction of High-Pressure Vapor-Liquid Equilibrium. *Journal of Advanced Research* 4 (2) : 137-145. <https://doi.org/10.1016/j.jare.2012.03.004>.
- [73] Xu X., Chen H., Liu C., and Dang C. 2019. Prediction of the Binary Interaction Parameter of Carbon Dioxide/Alkanes Mixtures in the Pseudocritical Region. *ACS Omega* 4 (8) : 13279-13294. <https://doi.org/10.1021/acsomega.9b01450>.
- [74] Pedersen K. S., Christensen P. L., and Shaikh J. A. 2014. *Phase Behavior of Petroleum Reservoir Fluids* (2nd Edition). Boca Raton, FL: CRC Press.
- [75] Cismondi M., Rodríguez-Reartes S.B., Milanésio J.M., and Zabaloy M. S. 2012. Phase Equilibria of CO₂ + n-Alkane Binary Systems in Wide Ranges of Conditions: Development of Predictive Correlations Based on Cubic Mixing Rules. *Industrial & Engineering Chemistry Research* 51 (17) : 6232-6250. <https://doi.org/10.1021/ie2018806>.
- [76] Kato K., Nagahama K., and Hirata M. 1981. Generalized Interaction Parameters for the Peng-Robinson Equation of State: Carbon Dioxide-n-Paraffin Binary Systems. *Fluid Phase Equilibria* 7 (3-4) : 219-231. [https://doi.org/10.1016/0378-3812\(81\)80009-X](https://doi.org/10.1016/0378-3812(81)80009-X).
- [77] Bae H. K., Nagahama K., and Hirata M. 1981. Measurement and Correlation of High Pressure Vapor-Liquid Equilibria for the Systems Ethylene-1-Butene and Ethylene-Propylene. *Journal of Chemical Engineering of Japan* 14 (1) : 1-6. <https://doi.org/10.1252/jcej.14.1>.
- [78] Elliott Daubert, T. E. Jr., 1985. Revised Procedures for Phase Equilibrium Calculations with the Soave Equation of State. *Industrial & Engineering Chemistry Process Design and Development*, 24(3), 743-748.
- [79] Valderrama J. O., Obaid-Ur-Rehman S., and Cisternas L. A. 1988. Generalized Interaction Parameters in Cubic Equations of State for CO₂-n-alkane Mixtures. *Fluid Phase Equilibria* 40 (3) : 217-233. [https://doi.org/10.1016/0378-3812\(88\)87019-5](https://doi.org/10.1016/0378-3812(88)87019-5).
- [80] Gao G., Daridon J., Saint Guirons H., Xans P., and Montel F. 1992. A Simple Correlation to Evaluate Binary Interaction Parameters of the Peng-Robinson Equation of State: Binary Light Hydrocarbon Systems. *Fluid Phase Equilibria* 74 (15) : 85-93. [https://doi.org/10.1016/0378-3812\(92\)85054-C](https://doi.org/10.1016/0378-3812(92)85054-C).
- [81] Kordas A., Tsoutsouras K., Stamataki S., and Tassios D. 1994. A Generalized Correlation for the Interaction Coefficients of CO₂-Hydrocarbon Binary Mixtures. *Fluid Phase Equilibria* 93: 141-166. [https://doi.org/10.1016/0378-3812\(94\)87006-3](https://doi.org/10.1016/0378-3812(94)87006-3).
- [82] Lee, M. J. Sun, H. C. 1992. Thermodynamic Property Predic-

- tions for Refrigerant Mixtures. *Industrial & Engineering Chemistry Research* 31: 1212-1216. <https://doi.org/10.1021/ie00004a036>.
- [83] Jaubert J. N. and Mutelet F. 2004. VLE Predictions with the Peng-Robinson Equation of State and Temperature Dependent k_{ij} Calculated through a Group Contribution Method. *Fluid Phase Equilibria* 224 (2): 285-304. <https://doi.org/10.1016/j.fluid.2004.06.059>.
- [84] Pedersen K. S., Milter J., and Sørensen H. 2004. Cubic Equations of State Applied to HT/HP and Highly Aromatic Fluids. *SPE Journal* 9 (2): 186-192. <https://doi.org/10.2118/88364-PA>.
- [85] Whitson C. H. and Brulé M. R. 2000. *Phase Behavior* (2nd Edition). SPE Monograph Series, Vol. 20, Richardson, TX.
- [86] Li X., Yang D., Zhang X., Zhang G., and Gao J., 2016. Binary Interaction Parameters of CO₂-Heavy-*n*-Alkanes Systems by Using Peng-Robinson Equation of State with Modified Alpha Function. *Fluid Phase Equilibria*, 417, 77-86. <https://doi.org/10.1016/j.fluid.2016.02.016>.
- [87] Huang D., Li X., and Yang D. 2020. Determination of Multiphase Boundaries for Pressure-Temperature (P-T) and Enthalpy-Temperature (H-T) Phase Diagrams of C₃H₈/CO₂/Water/Heavy Oil Systems at High Pressures and Elevated Temperatures. *Industrial & Engineering Chemistry Research* 59 (1): 423-436. <https://doi.org/10.1021/acs.iecr.9b05519>.
- [88] Li X., Li H., and Yang D. 2013. Determination of Multiphase Boundaries and Swelling Factors of Solvent(s)-CO₂-Heavy Oil Systems at High Pressures and Elevated Temperatures. *Energy & Fuels* 27 (3): 1293-1306. <https://doi.org/10.1021/ef301866e>.
- [89] Chen Z. and Yang D. 2020. A Tangent-Line Approach for Effective Density Used in Ideal Mixing Rule; Part II-Evaluation of Mixing Characteristics of Oil/Gas Systems and Application Criteria. *SPE Journal* 25 (6): 3160-3185. <https://doi.org/10.2118/200490-PA>.
- [90] Svrcek W. Y. and Mehrotra A. K. 1982. Gas Solubility, Viscosity, and Density Measurements for Athabasca Bitumen. *Journal of Canadian Petroleum Technology* 21 (4): 31-38. <https://doi.org/10.2118/82-04-02>.
- [91] Haddadnia A., Zirrahi M., Hassanzadeh H., and Abedi J. 2017. Solubility and Thermo-Physical Properties Measurement of CO₂- and N₂-Athabasca Bitumen Systems. *Journal of Petroleum Science and Engineering* 154: 277-283. <https://doi.org/10.1016/j.petrol.2017.04.035>.
- [92] Kariznovi M. 2013. *Phase Behaviour Study and Physical Properties Measurement for Athabasca Bitumen/Solvent Systems Applicable for Thermal and Hybrid Solvent Recovery Processes*. Ph. D. Dissertation, University of Calgary, Calgary, AB.
- [93] Zirrahi M., Hassanzadeh H., and Abedi J. 2017. Experimental and Modeling Studies of Water, Light *n*-alkanes and MacKay River Bitumen Ternary Systems. *Fuel* 196: 1-12. <https://doi.org/10.1016/j.fuel.2017.01.078>.
- [94] Ramos-Pallares F., Schoeggl F. F., Taylor S. D., Satyro M. A., and Yarranton H. W. 2015. Predicting the Viscosity of Hydrocarbon Mixtures and Diluted Heavy Oils Using the Expanded Fluid Model. *Energy & Fuels* 30 (3): 3575-3595. <https://doi.org/10.1021/acs.energyfuels.5b01951>.
- [95] Kariznovi M., Nourozieh H., and Abedi J. 2017. Vapor-Liquid Equilibrium of Bitumen-Ethane Mixtures for Three Athabasca Bitumen Samples. *Journal of Chemical & Engineering Data* 62 (5): 2198-2207. <https://doi.org/10.1021/acs.jced.7b00322>.
- [96] Argüelles-Vivas F. J., Babadagli T., Little L., Romaniuk N., and Ozum B. High Temperature Density, Viscosity, and Interfacial Tension Measurements of Bitumen-Pentane-Biodiesel and Process Water Mixtures. *Journal of Chemical Engineering Data* 2012, 57 (10): 2878-2889. <https://doi.org/10.1021/je3008217>.
- [97] Nourozieh H., Kariznovi M., and Abedi J. 2014. Measurement and Prediction of Density for the Mixture of Athabasca Bitumen and Pentane at Temperatures up to 200°C. *Energy & Fuels* 28 (5): 2874-2885. <https://doi.org/10.1021/ef4022784>.
- [98] Kariznovi M., Nourozieh H., and Abedi J. Volumetric Properties of Athabasca Bitumen + *n*-Hexane Mixtures. *Energy & Fuels* 2014, 28 (12): 7418-7425. <https://doi.org/10.1021/ef5019884>.
- [99] Haddadnia A., Zirrahi M., Hassanzadeh H., and Abedi J. 2018. Thermo-Physical Properties of *n*-Pentane/Bitumen and *n*-Pentane/Bitumen Mixture Systems. *The Canadian Journal of Chemical Engineering* 96 (1): 339-351. <https://doi.org/10.1002/cjce.22873>.
- [100] Haddadnia A., Azinfar B., Zirrahi M., Hassanzadeh H., and Abedi J. 2018. Thermophysical Properties of Dimethyl Ether/Athabasca Bitumen System. *The Canadian Journal of Chemical Engineering* 96 (2): 597-604. <https://doi.org/10.1002/cjce.23009>.
- [101] Freitag N. P. and Kristoff B. J. 1998. Comparison of Carbon Dioxide and Methane as Additives at Steamflood Conditions. *SPE Journal* 3 (1): 14-18. <https://doi.org/10.2118/30297-PA>.
- [102] Maczynski A., Shaw D., Goral M., Wisniewska-Gocłowska B., Skrzecz A., Maczynska Z., Owczarek I., Blazej K., Haulait-Pirson M. C., Kapuku F., Hefter G. T., and Szafranski A. 2005. IUPAC-NIST Solubility Data Series. 81. Hydrocarbons with Water and Seawater-Revised and Updated. Part 1. C₅ Hydrocarbons with Water. *Journal of Physical and Chemical Reference Data* 34 (2): 441-476. <https://doi.org/10.1063/1.1790005>.
- [103] Maczynski A., Shaw D., Goral M., Wisniewska-Gocłowska B., Skrzecz A., Owczarek I., Blazej K., Haulait-Pirson M. C., Hefter G. T., Maczynska Z., Szafranski A., Tsouopoulos C., and Young C. L. 2005. IUPAC-NIST Solubility Data Series. 81. Hydrocarbons with Water and Seawater-Revised and Updated. Part 2. Benzene with Water and Heavy Water. *Journal of Physical and Chemical Reference Data* 34 (2): 477-542. <https://doi.org/10.1063/1.1790006>.
- [104] Maczynski A., Shaw D., Goral M., Wisniewska-Gocłowska B., Skrzecz A., Owczarek I., Blazej K., Haulait-Pirson M. C., Hefter G. T., Maczynska Z., Szafranski A., and Young C. L. 2005. IUPAC-NIST Solubility Data Series. 81. Hydrocarbons with Water and Seawater Revised and Updated. Part 3. C₆H₈-C₆H₁₂ Hydrocarbons with Water and Heavy Water. *Journal of Physical and Chemical Reference Data* 34 (2): 657-708. <https://doi.org/10.1063/1.1796631>.
- [105] Maczynski A., Shaw D., Goral M., Wisniewska-Gocłowska B., Skrzecz A., Owczarek I., Blazej K., Haulait-Pirson M. C., Hefter G. T., Kapuku F., Maczynska Z., and Young C. L. 2005.

- IUPAC-NIST Solubility Data Series. 81. Hydrocarbons with Water and Seawater Revised and Updated. Part 4. C_6H_{14} Hydrocarbons with Water. Journal of Physical and Chemical Reference Data 34 (2): 709-713. <https://doi.org/10.1063/1.1796651>.
- [106] Maczynski A., Shaw D., Goral M., Wisniewska-Gocłowska B., Skrzecz A., Owczarek I., Blazej K., Haulait-Pirson M. C., Hefter G. T., Kapuku F., Maczynska Z., and Young C. L. 2005. IUPAC-NIST Solubility Data Series. 81. Hydrocarbons with Water and Seawater-Revised and Updated. Part 5. C_7 Hydrocarbons with Water and Heavy Water. Journal of Physical and Chemical Reference Data 34 (3): 1399-1487. <https://doi.org/10.1063/1.1840737>.
- [107] Shaw D., Maczynski A., Goral M., Wisniewska-Gocłowska B., Skrzecz A., Owczarek I., Blazej K., Haulait-Pirson M. C., Hefter G. T., Kapuku F., Maczynska Z., and Szafranski A. 2006. IUPAC-NIST Solubility Data Series. 81. Hydrocarbons with water and seawater-Revised and Updated. Part 10. C_{11} and C_{12} hydrocarbons with water. Journal of Physical and Chemical Reference Data 35 (1): 153-203. <https://doi.org/10.1063/1.2134730>.
- [108] Shaw D., Maczynski A., Goral M., Wisniewska-Gocłowska B., Skrzecz A., Owczarek I., Blazej K., Haulait-Pirson M. C., Hefter G. T., Huyskens P. L., Kapuku F., Maczynska Z., and Szafranski A. 2006. IUPAC-NIST Solubility Data Series. 81. Hydrocarbons with Water and Seawater-Revised and Updated. Part 9. C_{10} Hydrocarbons with Water. Journal of Physical and Chemical Reference Data 35 (1): 93-151. <https://doi.org/10.1063/1.2131103>.
- [109] Shaw D., Maczynski A., Goral M., Wisniewska-Gocłowska B., Skrzecz A., Owczarek I., Blazej K., Haulait-Pirson M. C., Hefter G. T., Kapuku F., Maczynska Z., and Szafranski A. 2006. IUPAC-NIST Solubility Data Series. 81. Hydrocarbons with Water and Seawater-Revised and Updated. Part 11. C_{13} - C_{36} Hydrocarbons with Water. Journal of Physical and Chemical Reference Data 35 (2): 687-784. <https://doi.org/10.1063/1.2132315>.
- [110] Shaw D., Maczynski A., Goral M., Wisniewska-Gocłowska B., Skrzecz A., Owczarek I., Blazej K., Haulait-Pirson M. C., Hefter G. T., Maczynska Z., and Szafranski A. 2005. IUPAC-NIST Solubility Data Series. 81. Hydrocarbons with Water and Seawater Revised and Updated. Part 6. C_8H_8 - C_8H_{10} Hydrocarbons with Water. Journal of Physical and Chemical Reference Data 34 (3): 1489-1553. <https://doi.org/10.1063/1.1839880>.
- [111] Shaw D., Maczynski A., Goral M., Wisniewska-Gocłowska B., Skrzecz A., Owczarek I., Blazej K., Haulait-Pirson M. C., Hefter G. T., Kapuku F., Maczynska Z., and Szafranski A. 2005. IUPAC-NIST Solubility Data Series. 81. Hydrocarbons with Water and Seawater Revised and Updated. Part 7. C_8H_{12} - C_8H_{18} Hydrocarbons with Water. Journal of Physical and Chemical Reference Data 34 (4): 2261-2298. <https://doi.org/10.1063/1.1842097>.
- [112] Shaw D., Maczynski A., Goral M., Wisniewska-Gocłowska B., Skrzecz A., Owczarek I., Blazej K., Haulait-Pirson M. C., Hefter G. T., Kapuku F., Maczynska Z., and Szafranski A. 2005. IUPAC-NIST Solubility Data Series. 81. Hydrocarbons with Water and Seawater-Revised and Updated. Part 8. C_9 Hydrocarbons with Water. Journal of Physical and Chemical Reference Data 34 (4): 2299-2345. <https://doi.org/10.1063/1.1842098>.
- [113] Kobayashi, R. and Katz, D. 1953. Vapor-Liquid Equilibria for Binary Hydrocarbon-Water Systems. Industrial & Engineering Chemistry, 45(2), 440-446.
- [114] Li, H. and Yang, D. 2016. Determination of Individual Diffusion Coefficients of Solvent/ CO_2 Mixture in Heavy Oil Using Pressure-Decay Method. SPE Journal 21 (1): 131-143. SPE-176032-PA. <https://doi.org/10.2118/176032-PA>.
- [115] Zheng S. and Yang D. 2017. Experimental and Theoretical Determination of Diffusion Coefficients of CO_2 -Heavy Oil Systems by Coupling Heat and Mass Transfer. Journal of Energy Resources Technology 139 (2): 022901. <https://doi.org/10.1115/1.4033982>.
- [116] Sun H., Li H., and Yang D. 2014. Coupling Heat and Mass Transfer for a Gas Mixture-Heavy Oil System at High Pressures and Elevated Temperatures. International Journal of Heat and Mass Transfer 74 (7): 173-184. <https://doi.org/10.1016/j.ijheat-masstransfer.2014.03.004>.
- [117] Zheng S. and Yang D. 2017. Determination of Individual Diffusion Coefficients of $C_3H_8/n-C_4H_{10}/CO_2$ /Heavy-Oil Systems at High Pressures and Elevated Temperatures by Dynamic Volume Analysis. SPE Journal 22 (3): 799-816. <https://doi.org/10.2118/179618-PA>.
- [118] Schmidt T. 1989. *Mass Transfer by Diffusion. AOSTRA Technical Handbook on Oil Sands, Bitumen and Heavy Oils*. Edmonton, AB: Alberta Oil Sand Technologies and Research Authority.
- [119] Upreti S. R. and Mehrotra A. K. 2002. Diffusivity of CO_2 , CH_4 , C_2H_6 and N_2 in Athabasca Bitumen. The Canadian Journal of Chemical Engineering 80 (1): 116-125. <https://doi.org/10.1002/cjce.5450800112>.
- [120] Etminan S. R., Maini B. B., Chen Z., and Hassanzadeh H. 2010. Constant-Pressure Technique for Gas Diffusivity and Solubility Measurements in Heavy Oil and Bitumen. Energy & Fuels 24 (1): 533-549. <https://doi.org/10.1021/ef9008955>.
- [121] Fadaei H., Scarff B., and Sinton D. 2011. Rapid Microfluidics-Based Measurement of CO_2 Diffusivity in Bitumen. Energy & Fuels 25 (10): 4829-4835. <https://doi.org/10.1021/ef2009265>.
- [122] Tharanivasan A. K., Yang C., and Gu Y. 2006. Measurements of Molecular Diffusion Coefficients of Carbon Dioxide, Methane, and Propane in Heavy Oil under Reservoir Conditions. Energy & Fuels 20 (6): 2509-2517. <https://doi.org/10.1021/ef060080d>.
- [123] Yang C. and Gu Y. 2006. Diffusion Coefficients and Oil Swelling Factors of Carbon Dioxide, Methane, Ethane, Propane, and Their Mixtures in Heavy Oil. Fluid Phase Equilibria 243 (1-2): 64-73. <https://doi.org/10.1016/j.fluid.2006.02.020>.
- [124] Jang H. W. and Yang D. 2020. Determination of Concentration-Dependent Gas Diffusivity in Reservoir Fluid Systems. Industrial & Engineering Chemistry Research 59 (33): 15028-15047. <https://doi.org/10.1021/acs.iecr.0c01847>.
- [125] Jang H. W. and Yang D. 2021. Determination of Individual Concentration-Dependent Diffusivity of the Binary Gas-

- Mixtures in Reservoir-Fluid Systems. *International Journal of Heat and Mass Transfer* 181: 121867. <https://doi.org/10.1016/j.ijheatmasstransfer.2021.121867>.
- [126] Jang H. W., and Yang D. 2021. Determination of Main-Term and Cross-Term Gas Diffusivities in Heavy Oil Systems Considering Local Oil Swelling Effect. *Journal of Energy Resources Technology* 143 (2): 023003. <https://doi.org/10.1115/1.4047764>.
- [127] Luo P., Yang C., and Gu Y. 2007. Enhanced Solvent Dissolution into In-Situ Upgraded Heavy Oil under Different Pressures. *Fluid Phase Equilibria* 252 (1-2): 143-151. <https://doi.org/10.1016/j.fluid.2007.01.005>.
- [128] Ganapathi K. 2009. *Solubility and Diffusivity Study for Light Gases in Heavy Oil and Its Fractions*. M.A.Sc. Thesis, University of Regina, Regina, SK.
- [129] Etmnan S. R., Maini B. B., and Chen Z. 2014. Modeling the Diffusion Controlled Swelling and Determination of Molecular Diffusion Coefficient in Propane-Bitumen System Using a Front Tracking Moving Boundary Technique. Paper SPE-170182-MS, presented at the SPE Heavy Oil Conference, Calgary, AB, 10-12 June. <https://doi.org/10.2118/170182-MS>.
- [130] Marufuzzaman M. 2010. *Solubility and Diffusivity of Carbon Dioxide, Ethane and Propane in Heavy Oil and Its SARA Fractions*. M.A.Sc. Thesis, University of Regina, Regina, SK.
- [131] Zheng S., Sun H., and Yang D. 2016. Coupling Heat and Mass Transfer for Determining Individual Diffusion Coefficient of A Hot C₃H₈-CO₂ Mixture in Heavy Oil under Reservoir Conditions. *International Journal of Heat and Mass Transfer* 102: 251-263. <https://doi.org/10.1016/j.ijheatmasstransfer.2016.05.136>.
- [132] Shi Y., Li X., and Yang D. 2016. Nonequilibrium Phase Behaviour of Alkane Solvent(s)-CO₂-Heavy Oil Systems under Reservoir Conditions. *Industrial & Engineering Chemistry Research* 55 (10): 2860-2871. <https://doi.org/10.1021/acs.iecr.5b04831>.
- [133] Shi, Y. and Yang, D. 2017. Experimental and Theoretical Quantification of Non-equilibrium Phase Behaviour and Physical Properties of Foamy Oil under Reservoir Conditions. *Journal of Energy Resources Technology* 139 (6): 062902. <https://doi.org/10.1115/1.4036960>.
- [134] Shi, Y. and Yang, D. 2017. Non-equilibrium Phase Behaviour and Mass Transfer of Alkane Solvent (s) -CO₂-Heavy Oil Systems under Reservoir Conditions. Presented at the 25th Williston Basin Petroleum Conference, Regina, SK, 2-4 May. <https://doi.org/10.1021/acs.iecr.5b04831>.
- [135] Shi, Y. and Yang, D. 2017. Quantification of a Single Gas Bubble Growth in Solvent(s)-CO₂-Heavy Oil Systems with Consideration of Multicomponent Diffusion under Non-equilibrium Conditions. *Journal of Energy Resources Technology* 139 (2): 022908. <https://doi.org/10.1115/1.4035150>.
- [136] Shi Y., Li X., and Yang D. 2015. Experimental and theoretical determination of foamy oil properties under non-equilibrium conditions. Presented at the 36th IEA-EOR Collaborative Project Workshop & Symposium, Sapporo, Japan, 9-11 September.
- [137] Lopez-Echeverry J. S., Reif-Acherman S., and Araujo-Lopez E. 2017. Peng-Robinson Equation of State: 40 Years through Cubics. *Fluid Phase Equilibria* 447: 39-71. <https://doi.org/10.1016/j.fluid.2017.05.007>.
- [138] Gasem K. A. M., Gao W., Pan Z., and Robinson, Jr., R. L. 2001. A Modified Temperature Dependence for the Peng-Robinson Equation of State. *Fluid Phase Equilibria* 181 (1-2): 113-125. [https://doi.org/10.1016/S0378-3812\(01\)00488-5](https://doi.org/10.1016/S0378-3812(01)00488-5).
- [139] Atonge E.A. and Yang D., 2023. Comparative Evaluation of α Functions and Volume-Translation (VT) Strategies to Predict Densities for Gas (es)-Heavy Oil/Bitumen Systems. *SPE Journal*, preprint, <https://doi.org/10.2118/217980-PA>.
- [140] Atonge E.A. and Yang D., 2023. Comparative Evaluation of α Functions for Soave-Redlich-Kwong Equation of State (EOS) and Peng-Robinson EOS to Predict Saturation Pressures for Gas (es)-Heavy Oil/Bitumen-Water Systems. *SPE Reservoir Evaluation & Engineering*, 26 (4): 1323-1343., <https://doi.org/10.2118/215835-PA>.
- [141] Economou I. G. and Tsonopoulos C. Associating Models and Mixing Rules in Equations of State for Water/Hydrocarbon Mixtures. *Chemical Engineering Science* 1997, 52 (4): 511-525. [https://doi.org/10.1016/S0009-2509\(96\)00441-1](https://doi.org/10.1016/S0009-2509(96)00441-1).
- [142] Yushchenko T. S. and Brusilovsky A. I. 2016. Mathematical Modeling of Gas-Condensate Mixture PVT-Properties Including Presence of Brine in Reservoir. *Fluid Phase Equilibria* 409: 37-48. <https://doi.org/10.1016/j.fluid.2015.09.029>.
- [143] Huron M. J. and Vidal J. 1979. New Mixing Rules in Simple Equations of State for Representing Vapour-Liquid Equilibria of Strongly Non-Ideal Mixtures. *Fluid Phase Equilibria* 3 (4): 255-271. [https://doi.org/10.1016/0378-3812\(79\)80001-1](https://doi.org/10.1016/0378-3812(79)80001-1).
- [144] Li X., Yang D., and Fan Z. 2014. Phase Behaviour and Viscosity Reduction of CO₂-Heavy Oil Systems at High Pressures and Elevated Temperatures. Paper SPE-170057-MS, presented at the SPE Canada Heavy Oil Conference, Calgary, AB, 10-12 June. <https://doi.org/10.2118/170057-MS>.
- [145] Li X. 2015. *Phase Behaviour of Alkane Solvent (s)-CO₂-Water-Heavy Oil Systems at High Pressures and Elevated Temperatures*. Ph.D. Dissertation, University of Regina, Regina, SK.
- [146] Huang D. 2020. *Phase Behaviour of Solvent (s)/Water/Heavy Oil Systems at High Pressures and Elevated Temperatures Based on Isoenthalpic Flash*. Ph.D. Dissertation, University of Regina, Regina, SK.
- [147] Huang D., Li Y., and Yang D. 2023 Phase Behavior and Physical Properties of Dimethyl Ether/CO₂/Water/Heavy Oil Systems under Reservoir Conditions. *SPE Journal*, 28 (1): 301-318.
- [148] Pénélox A., Rauzy E., and Fréze R. 1982. A Consistent Correction for Redlich-Kwong-Soave Volumes. *Fluid Phase Equilibria*, 8(1), 7-23.
- [149] Saryazdi F. 2012. *Density Prediction for Mixtures of Heavy Oil and Solvents*. MSc Thesis, University of Calgary, Calgary, AB.
- [150] Saryazdi F., Motahhari H., Schoegl F.F., Taylor S.D., and Yarranton H.W. 2013. Density of Hydrocarbon Mixtures and Bitumen Diluted with Solvents and Dissolved Gases. *Energy & Fuels* 27(7), 3666-3678.
- [151] Nourozieh H., Kariznovi M., and Abedi J. 2015. Viscosity Measurement and Modeling for Mixtures of Athabasca Bitumen/n-Pentane at Temperatures up to 200°C. *SPE Journal* 20 (2): 226-

238. <https://doi.org/10.2118/170252-PA>.
- [152] Nourozieh H., Kariznovi M., and Abedi J. 2015. Viscosity Measurement and Modeling for Mixtures of Athabasca Bitumen/Hexane. *Journal of Petroleum Science and Engineering* 129: 159-167. <https://doi.org/10.1016/j.petrol.2015.03.002>.
- [153] Chen, Z., Li, X., and Yang, D. Quantification of Viscosity for Solvents-Heavy Oil/Bitumen Systems in the Presence of Water at High Pressures and Elevated Temperatures. *Industrial & Engineering Chemistry Research* 2019, 58 (2) : 1044-1054. <https://doi.org/10.1021/acs.iecr.8b04679>.
- [154] Chen Z. 2019. *Quantification of Phase Behaviour and Physical Properties of Solvents-Heavy Oil/Bitumen-Water Systems at High Pressures and Elevated Temperatures*. Ph.D. Dissertation, University of Regina, Regina, SK.
- [155] Hu B. and Yang D. Viscosity Modeling of Solvent (s) -Water-Heavy Oil/Bitumen Systems at High Pressures and Elevated Temperatures. Paper SPE-219354-MS, presented at the SPE Gas & Oil Technology Showcase and Conference (GOTECH) , Dubai, UAE, May 7-9, 2024.
- [156] Hu B. and Yang D. Viscosity Modeling of Solvent (s) -Heavy Oil/bitumen Systems at High Pressures and Elevated Temperatures. Paper OMAE2024-125089, presented at the ASME Ocean Offshore and Arctic Engineering OMAE Conference, Singapore, June 9-14, 2024.
- [157] Zheng S., Li H., Sun H., and Yang D. 2016. Determination of Diffusion Coefficient for Alkane Solvent-CO₂ Mixtures in Heavy Oil with Consideration of Swelling Effect. *Industrial & Engineering Chemistry Research* 55 (6) : 1533-1549. <https://doi.org/10.1021/acs.iecr.5b03929>.
- [158] Jang H. W. and Yang D. 2022. Determination of Effective Diffusivity of Each Component of a Binary Gas-Mixture in Porous Media Saturated with Heavy Oil. *International Journal of Mass and Heat Transfer* 184: 122332. <https://doi.org/10.1016/j.ijheatmasstransfer.2021.122332>.
- [159] Zheng S. 2016. *Enhanced Heat and Mass Transfer for Alkane Solvent (s) -CO₂-Heavy Oil Systems at High Pressures and Elevated Temperatures*. Ph.D. Dissertation, University of Regina, Regina, SK.
- [160] Zhao W., Jang H. W., and Yang D., 2023. Determination of Concentration-Dependent Effective Diffusivity of Each Gas Component of a Binary Mixture in Porous Media Saturated with Heavy Oil under Reservoir Conditions. *SPE Reservoir Evaluation & Engineering*, 26 (4): 1197-1211 . <https://doi.org/10.2118/215832-PA>.
- [161] Jang H. W., and Yang D., 2023. Determination of the Concentration-Dependent Effective Diffusivity of CO₂ in Unconsolidated Porous Media Saturated with Heavy Oil by Considering the Swelling Effect. *International Journal of Heat and Mass Transfer*, 201 (Part 2) , 123552. <https://doi.org/10.1016/j.ijheatmasstransfer.2022.123552>
- [162] Shi Y., Zheng S., and Yang D. 2017. Determination of Individual Diffusion Coefficients of Solvents-CO₂-Heavy Oil Systems with Consideration of Natural Convection Induced by Swelling Effect. *International Journal of Heat and Mass Transfer* 107: 572-585. <https://doi.org/10.1016/j.ijheatmasstransfer.2016.11.060>.
- [163] Shi Y. 2017. *Nonequilibrium Phase Behaviour and Mass Transfer of Alkane Solvents (s) -CO₂-Heavy Oil Systems Under Reservoir Conditions*. Ph.D. Dissertation, University of Regina, Regina, SK.
- [164] Shi Y., Zhao W., Li S., and Yang D. Quantification of Gas Exsolution and Preferential Diffusion for Alkane Solvent (s) -CO₂-Heavy Oil Systems under Nonequilibrium Conditions. *Journal of Petroleum Science and Engineering* 2022, 208 (Part A) : 109283. <https://doi.org/10.1016/j.petrol.2021.109283>
- [165] Zhao Z., Shi Y., Yang D., and Jia N. Quantification of Gas Exsolution of Alkane Solvents-CO₂ Mixture in Heavy Oil with Consideration of Individual Interface Resistance under Nonequilibrium Conditions. *Journal of Petroleum Science and Engineering* 2019, 180: 1112-1123. <https://doi.org/10.1016/j.petrol.2019.05.058>.
- [166] Dong X., Zhao Z., Yang D., and Jia N. Quantification of Gas Exsolution Dynamics for CO₂/CH₄-Heavy Oil Systems with Population Balance Equations. Paper SPE-218070-MS, presented at the SPE Canadian Energy Technology Conference and Exhibition, Calgary, AB, March 13-14, 2024.

Daoyong Yang is a professor of Energy Systems Engineering for the Faculty of Engineering and Applied Science at the University of Regina. His major research areas include reservoir description and dynamics, phase behaviour, mass and heat transfer, assisted history matching, formation evaluation, production optimization, CO₂ EOR and storage, transient pressure/rate analysis, reservoir nanoagents, jet dynamics, artificial-lift methods, transport phenomena, interfacial interactions in EOR processes, heavy-oil recovery, unconventional resources exploitation, and oilfield wastewater treatment. He has authored or coauthored 201 refereed-journal articles and 140 conference papers and holds three patents. Yang holds BSc and PhD degrees in petroleum engineering from the China University of Petroleum (East China) and a PhD degree in petroleum systems engineering from the University of Regina. He is a member of SPE, ACS, Society of Exploration Geophysicists (SEG), American Society of Mechanical Engineers (ASME), and Society of Petrophysicists and Well Log Analysts (SPWLA) and is a registered professional engineer with the Association of Professional Engineers and Geoscientists of Saskatchewan (APEGS), Canada.